Progress In Electromagnetics Research, Vol. 168, 87–111, 2020

Multiple Scattering of Waves by Complex Objects Using Hybrid Method of T-Matrix and Foldy-Lax Equations Using Vector Spherical Waves and Vector Spheroidal Waves

Huanting Huang[1, *], Leung Tsang[1], Andreas Colliander[2], Rashmi Shah[2], Xiaolan Xu[2], and Simon Yueh[2]

Abstract—In this paper, we develop numerical methods for using vector spherical and spheroidal waves in the hybrid method to calculate the multiple scattering of objects of complex shapes, based on the rigorous solutions of Maxwell equations in the form of Foldy-Lax multiple scattering equations (FL). The steps in the hybrid method are: (1) calculating the T-matrix of each single object using vector spherical/spheroidal waves and (2) vector spherical/spheroidal waves addition theorem. We utilize the commercial software HFSS to calculate the scattered fields of a complex object on the circumscribing sphere or spheroid for multiple incidences and polarizations. The T-matrix of spherical waves or spheroidal waves are then obtained from these scattered fields. To perform wave transformations (i.e., addition theorem) for vector spherical/spheroidal waves, we develop robust numerical methods. Numerical results are illustrated for T-matrices and numerical vector addition theorems.

1. INTRODUCTION

Multiple scattering of waves by discrete scatterers have been studied extensively using analytical theory of radiative transfer equation (RTE) [1–6], distorted Born approximation (DBA) [7–10] and Feynman diagrammatic methods [11–13]. The effects of multiple scattering influence the transmission properties and bistatic scattering properties of a conglomeration of objects. With the advent of computers and computational methods, full wave simulations of multiple scattering of 3 dimensional solutions of Maxwell equations have become a topic of current interests [14–19]. Recently, it has been shown by the Numerical Solutions of 3D Maxwell Equations (NMM3D) full-wave simulations that the attenuation of vegetation layer can be significantly overestimated by the classical RTE and DBA [18, 19]. This is because the classical models assume that vegetation is spatially homogeneous with a uniform statistical distribution in position [1, 7, 20]. The uniform distributions lead to the concept of an effective/average medium which is homogeneous. The homogeneous medium is similar to the "cloud model" and gives an effective attenuation rate and transmission that is homogeneous. Many kinds of vegetation, including agriculture crops, could have leaves, stems and branches distributed in clusters with substantial gaps between them. Thus, vegetation canopies are not homogeneous. Also, the transmissions in gaps are larger than that in non-gaps invalidating the homogeneous assumption of RTE and DBA [21].

A common approach in multiple scattering has been based on Foldy-Lax multiple scattering equations which are formulated using the T-matrix of single objects and translational additional theorem [1, 12, 15, 22, 23]. In the past, the objects are assumed to be of spherical shape or of cylindrical shape [12, 16, 17, 19, 24, 25]. The vector translation addition theorem is that of spherical

Received 4 August 2020, Accepted 5 October 2020, Scheduled 15 October 2020
* Corresponding author: Huanting Huang (huanght@umich.edu).
[1] Radiation Laboratory, Department of Electrical Engineering and Computer Science, The University of Michigan, Ann Arbor, MI 48109, USA. [2] Jet Propulsion Laboratory, California Institute of Technology, Pasadena, CA 91109, USA.

waves and cylindrical waves [12, 19]. The scattering of plane waves by quasi-homogeneous scatterers is investigated in [26]. The field coefficients are expressed via the T-matrix method with the best linear approximation [26]. It is shown that the far-field pattern of the quasi-homogeneous scatterer is decomposed into that of the respective homogeneous scatterer plus the perturbation far-field pattern, depending only on the deviations of the wavenumber profile function from the average value [26]. In comparison, the method developed in our paper is applicable to both quasi-homogeneous scatterers and inhomogeneous scatterers. The multiple scattering of 2D objects is calculated using the scattering operator method (SOM) in [27]. The technique presented in our paper is suitable to treat multiple scatterings of N 3D objects of complicated shapes where N is an arbitrary number (if additional scatterers are added, the value of N is increased). This technique has the same advantages as SOM [27] such as stability when compared with the integral method. We have extended the previous vector spherical waves method of Foldy-Lax to vector spheroidal wave expansions which are suitable for complicated 3D objects which can be enclosed by prolate spheroidal surfaces. In inverse scattering problem, reference [28] developed a novel inverse method to calculate the permittivity of an electrically small rod. The field across surface of the electrically small rod is assumed be constant. Based on this assumption, the closed-form solutions of the permittivity are derived from the scattering integral [28]. Reference [29] reconstructed the shapes and locations of multiple 3D perfect electric conducting (PEC) objects using the level set method. In our paper, the Foldy-Lax multiple scattering equations are efficient and accurate to solve the scatterings from multiple objects, especially when the fractional volume of the objects is small (e.g., vegetation canopy). In the future, for inverse scattering of the multiple scattering problems, we will use the hybrid method for the forward solution, and machine leaning techniques such as convolution neural network can be employed for inverse scattering [30].

In full wave simulations of multiple scattering in vegetation, the additional challenges are that the objects are of complex shapes consisting of branches and leaves and they are clustered together. For example, in microwave remote sensing of soil moisture and vegetation, the scattering objects are vegetation such as wheat, soya bean and corn that lies above the soils. In this paper, we use a hybrid method for NMM3D simulations of multiple scatterings by complex objects. In the hybrid method, the solutions are divided into the interior regions and the exterior regions. The complex object is placed in the interior region which has a circumscribing/enclosing boundary. The first step consists of solving Maxwell equations in the interior region. Off the-shelf technique of HFSS (high frequency structure simulator) or FEKO (field calculations involving bodies of arbitrary shape) is used to calculate the scattered fields of the complex object on the circumscribing boundary. In the next step, the T-matrices of the complex objects are then used in Foldy-Lax multiple scattering equations with the translational addition theorem.

In this paper, for the interior regions, we use circumscribing spheres and circumscribing spheroids. For the case of circumscribing spheres, we used vector spherical wave expansions [31]. For the case of circumscribing spheroids, we used vector spheroidal waves [32] expansions. Recently, we have also used circumscribing cylinders of infinite lengths [19, 21, 33]. To extract the T-matrix for an arbitrary-shape object, the off the-shelf technique HFSS is used. HFSS enables us to perform full-wave simulations of single objects with complicated structures. To calculate the T-matrix of the single object from HFSS, we first define a spherical/spheroidal surface (S) which encloses the object. Then, we excite the object using incident plane waves at different incident angles and polarizations in HFSS. Using the scattered field values from HFSS on the circumscribing boundary, the spherical/spheroidal wave expansion coefficients of the scattered waves are obtained. Since the expansion coefficients of the incident plane waves are known, the T-matrix is calculated from the scattered fields of HFSS. Analytic expressions of translational addition theorem of vector spherical waves are well established using Wigner 3-j coefficients [1]. The expressions of translational addition theorem of vector spheroid waves are very complicated and have only been implemented numerically for low order spheroidal waves [34–36]. In this paper, we develop robust numerical methods to calculate the coefficients of the translation addition theorem for vector spheroidal waves.

A short 3-page version of this present paper was presented at the ICCEM conference [37]. A longer version was in the PhD thesis of the first author [33]. The outline of the present paper is as follows. In Section 2, the numerical method of extracting T-matrix for complex objects using HFSS for vector spherical waves and vector spheroidal waves is developed. Section 3 presents the results and validation

for the numerical extraction of T-matrix. In Section 4, we describe the details of the methods for calculating the translation addition theorem numerically for vector spheroidal waves. Section 5 presents the results and discussions on the numerical translation addition method.

2. FOLDY-LAX MULTIPLE SCATTERING EQUATIONS

2.1. Foldy-Lax Multiple Scattering Equations and T-Matrix

In NMM3D full wave simulations, Maxwell equations are solved using the Foldy-Lax multiple scattering equations (FL) with generalized T-matrix. Consider an incident wave $\bar{E}_{inc}$ incident on N number of scatterers. In Foldy-Lax equations, one considers $\bar{E}^m_{ex}$, the final exciting field of scatterer m. The coupled equations for N number of scatterers with N final exciting fields, $\bar{E}^n_{ex}$, $n = 1, 2, 3, \ldots, N$ are (Fig. 1)

$$\bar{E}^m_{ex} = \bar{E}_{inc} + \sum_{\substack{n=1 \\ n\neq M}}^{N} \bar{\bar{G}}_{mn}\bar{\bar{T}}^n\bar{E}^n_{ex} \tag{1}$$

where $\bar{\bar{T}}^n$ is the generalized T-matrix of scatterer n, and $\bar{\bar{G}}_{mn}$ is the propagation of wave from scatterer n to scatterer m. The product $\bar{\bar{G}}_{mn}\bar{\bar{T}}^n\bar{E}^n_{ex}$ gives the scattered wave from scatterer n to scatterer m. The T-matrix describes the scattering of the object. In this paper, it is expressed in vector spherical waves and in vector spheroidal waves.

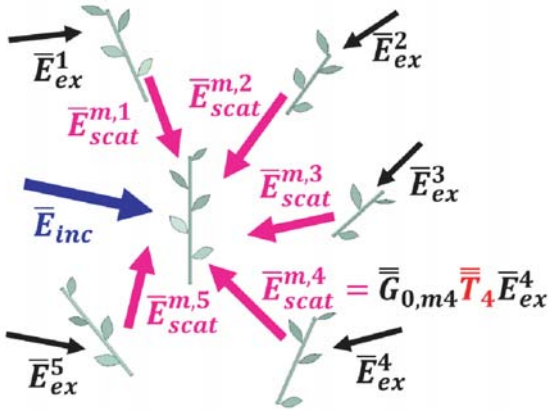

Figure 1. Illustration of Foldy-Lax multiple scattering equations using five branches.

For quasi-homogeneous scattering, the Foldy-Lax multiple scattering equations can be simplified by applying the Born approximation. The solutions of the Foldy-Lax multiple scattering equations require only one iteration for convergence [10]. The idea is similar to that of [38, 39].

2.2. Numerical T-matrix Extraction

The exciting fields are expanded in regular vector waves while the scattered waves outside the enclosing surface are expressed with outgoing vector waves (Fig. 2). Then, the T-matrix describes the linear relation between scattering field coefficients and the exciting field coefficients [1].

$$\begin{bmatrix} \bar{a}^{S(M)} \\ \bar{a}^{S(N)} \end{bmatrix} = \begin{bmatrix} \bar{\bar{T}}^{(11)} & \bar{\bar{T}}^{(12)} \\ \bar{\bar{T}}^{(21)} & \bar{\bar{T}}^{(22)} \end{bmatrix} \begin{bmatrix} \bar{a}^{E(M)} \\ \bar{a}^{E(N)} \end{bmatrix} = \bar{T} \begin{bmatrix} \bar{a}^{E(M)} \\ \bar{a}^{E(N)} \end{bmatrix} \tag{2}$$

In Equation (2), (M) and (N) stand for vector waves of the two polarizations; $\bar{a}^{E(M)}$ and $\bar{a}^{E(N)}$ represent the exciting field coefficients; and $\bar{a}^{S(M)}$ and $\bar{a}^{S(N)}$ represent the scattered field coefficients. For vector spherical waves, $N_{\max}$ is the number of multipoles for both M and N and $L_{\max} = N_{\max}(N_{\max} + 2)$ [1]. For spheroidal waves, we use separate $M_{\max}$ and $N_{\max}$, and

Figure 2. Two branches, each enclosed by a spherical surface (left figure) and a spheroidal surface (right figure), without overlap. The technique presented in this paper is suitable to treat any number of scatterers even though only two branches are shown in each sub figure.

$L_{\max} = N_{\max}(M_{\max} + 1)$. Thus, the dimensions of $\bar{a}^{E(M)}$, $\bar{a}^{E(N)}$, $\bar{a}^{S(M)}$, and $\bar{a}^{S(N)}$ are $L_{\max} \times 1$. Then $\bar{\bar{T}}^{(11)}$, $\bar{\bar{T}}^{(12)}$, $\bar{\bar{T}}^{(21)}$, and $\bar{\bar{T}}^{(22)}$ are of dimensions $L_{\max} \times L_{\max}$.

Let

$$\bar{\bar{T}} = \begin{bmatrix} \bar{\bar{T}}^{(11)} & \bar{\bar{T}}^{(12)} \\ \bar{\bar{T}}^{(21)} & \bar{\bar{T}}^{(22)} \end{bmatrix} \tag{3}$$

be the T-matrix. The size of the T-matrix ($\bar{\bar{T}}$) is $2L_{\max} \times 2L_{\max}$.

To find $\bar{\bar{T}}$ numerically for complex objects, the scatterer is excited with $2L_{\max}$ different incident plane waves (different incident angles and polarizations). For each of the plane wave incident wave, for example, the incident wave, we calculate $\bar{a}_l^{E(M)}$, $\bar{a}_l^{E(N)}$, for vector spherical waves or vector spheroidal waves. For each plane incident wave wave , the near scattered fields can be calculated using off-the-shelf techniques such as HFSS, FEKO, and CST. In this paper we used HFSS. The near scattered fields $\bar{E}^S(\bar{r})$ are calculated on the surfaces of smallest circumscribing sphere or spheroid respectively for vector spherical waves and vector spheroidal waves. Then, the scattered field coefficients are calculated by integration of the product of the $\bar{E}^S(\bar{r})$ and the vector spherical waves or vector spheroidal waves on the surfaces. Then, $\bar{a}_l^{S(M)}$, $\bar{a}_l^{S(N)}$ for vector spherical waves or vector spheroidal waves are calculated. These are repeated for $j = 1, 2 \ldots, 2L_{\max}$ incident plane waves.

These coefficients are assembled into the exciting field coefficient matrices and the scattered field coefficient matrices of sizes $2L_{\max} \times 2L_{\max}$ as follows.

$$\begin{bmatrix} \bar{a}_1^{E(M)} & \ldots & \bar{a}_{2L_{\max}}^{E(M)} \\ \bar{a}_1^{E(N)} & \ldots & \bar{a}_{2L_{\max}}^{E(N)} \end{bmatrix} \tag{4}$$

and

$$\begin{bmatrix} \bar{a}_1^{S(M)} & \ldots & \bar{a}_{2L_{\max}}^{S(M)} \\ \bar{a}_1^{S(N)} & \ldots & \bar{a}_{2L_{\max}}^{S(N)} \end{bmatrix} \tag{5}$$

Using these two coefficient matrices, then the $\bar{\bar{T}}$ of size $2L_{\max} \times 2L_{\max}$ is obtained by

$$\bar{\bar{T}} = \begin{bmatrix} \bar{a}_1^{S(M)} & \ldots & \bar{a}_{2L_{\max}}^{S(M)} \\ \bar{a}_1^{S(N)} & \ldots & \bar{a}_{2L_{\max}}^{S(N)} \end{bmatrix} \begin{bmatrix} \bar{a}_1^{E(M)} & \ldots & \bar{a}_{2L_{\max}}^{E(M)} \\ \bar{a}_1^{E(N)} & \ldots & \bar{a}_{2L_{\max}}^{E(N)} \end{bmatrix}^{-1} \tag{6}$$

The numerical methods to calculate the scattered field coefficients for vector spherical and spheroidal waves are described below.

2.3. Calculations of $\bar{a}_l^S$ and the T-Matrix for Vector Spherical Waves

Scattered fields are expressed in terms of vector spherical waves as below.

$$\bar{E}^S(\bar{r}) = \sum_{m,n} \begin{bmatrix} a_{mn}^{S(M)} \bar{M}_{mn}(kr, \theta, \phi) \\ +a_{mn}^{S(N)} \bar{N}_{mn}(kr, \theta, \phi) \end{bmatrix} \tag{7}$$

where $\bar{M}$ and $\bar{N}$ are as defined in page 27–28 of [31].

We use HFSS to calculate the tangential components of the scattered field on the surface of the circumscribing sphere of radius R. The scattered field expansion coefficients can be obtained using

$$a_{mn}^{S(M)} = [\gamma_{mn} h_n(kR) z_{2mn}]^{-1} \int_0^{\pi} d\theta \sin\theta \int_0^{2\pi} d\phi \hat{r} \times \bar{E}^s(R,\theta,\phi) \cdot \bar{B}_{-mn}(\theta,\phi) \tag{8}$$

$$a_{mn}^{S(N)} = \left[\gamma_{mn} \frac{[kRh_n(kR)]'}{kR} z_{3mn}\right]^{-1} \int_0^{\pi} d\theta \sin\theta \int_0^{2\pi} d\phi \hat{r} \times \bar{E}^s(R,\theta,\phi) \cdot \bar{C}_{-mn}(\theta,\phi) \tag{9}$$

For incident plane waves $\bar{E}_i = E_{pi}\hat{p}_i e^{i\bar{k}_i \cdot \bar{r}}$, the vector spherical wave expansion coefficients are [1]

$$a_{mn}^{E(M)} = (-1)^m \frac{(2n+1)}{\gamma_{mn} n(n+1)} i^n \left[E_{pi}\left(\hat{p}_i \cdot \bar{C}_{-mn}(\theta_i,\phi_i)\right)\right] \tag{10}$$

$$a_{mn}^{E(N)} = (-1)^m \frac{(2n+1)}{\gamma_{mn} n(n+1)} i^n \left[E_{pi}\left(\hat{p}_i \cdot \left(-i\bar{B}_{-mn}(\theta_i,\phi_i)\right)\right)\right] \tag{11}$$

where the superscript "E" means exciting fields. $\hat{p}_i$ is the polarization (either $\hat{v}$ or $\hat{h}$).

The expressions for both the scattered fields (Equations (8) and (9)) and incident fields (Equations (10) and (11)) are obtained. From these, the T-matrix with vector spherical wave expansions for a complex object is obtained using Equation (6). It is noted that this numerical method of extracting T-matrix works for the object with arbitrary shape. Then, the scattered field coefficients are obtained, and the T-matrix is extracted.

2.4. Numerical T-Matrix Extraction for Vector Spheroidal Waves

2.4.1. Calculations of $\bar{a}_l^S$ for Vector Spheroidal Waves

For vector spheroidal waves, there is no orthogonality property. Calculating the scattered field expansion coefficients are more complicated than that for the vector spherical waves.

Using the even and odd modes, the scattered field is expanded as

$$\bar{E}^s = \sum_{m,n} \left[a_{mn}^{S(M),e} \bar{M}_{e,mn}^{a(3)} + a_{mn}^{S(M),o} \bar{M}_{o,mn}^{a(3)} + a_{mn}^{S(N),e} \bar{N}_{e,mn}^{a(3)} + a_{mn}^{S(N),o} \bar{N}_{o,mn}^{a(3)}\right] \tag{12}$$

where "e" stands for the even mode, and "o" stands for the odd mode. The superscript "(3)" means the vector spheroidal waves of the third kind, which is the outgoing vector spheroidal waves. The definition of the superscript "a" is in Appendix. In this paper, $a = r$. The spheroidal waves are listed in the Appendix. The m index denotes the usual $\sin m\phi$ and $\cos m\phi$. The n index denotes the η variable which roughly corresponds to θ in the case of spherical waves. $\bar{E}^s$ is obtained from HFSS for a given incident wave. To calculate the scattered field coefficients a^s, we take the tangential $\bar{E}^s$ dot product with vector spheroidal waves and perform 2D numerical integration over the enclosing spheroidal surface.

To illustrate, we take $\widehat{\xi}\times$ of the above Equation (12), and then take the dot product with $\bar{M}_{e,m'n'}^{a(3)}$

$$\hat{\xi} \times \bar{E}^s \cdot \bar{M}_{e,m'n'}^{a(3)} = \sum_{m,n} \left[\begin{array}{l} a_{mn}^{S(M),e} \hat{\xi} \times \bar{M}_{e,mn}^{a(3)} \cdot \bar{M}_{e,m'n'}^{a(3)} + a_{mn}^{S(M),o} \hat{\xi} \times \bar{M}_{o,mn}^{a(3)} \cdot \bar{M}_{e,m'n'}^{a(3)} \\ + a_{mn}^{S(N),e} \hat{\xi} \times \bar{N}_{e,mn}^{a(3)} \cdot \bar{M}_{e,m'n'}^{a(3)} + a_{mn}^{S(N),o} \hat{\xi} \times \bar{N}_{o,mn}^{a(3)} \cdot \bar{M}_{e,m'n'}^{a(3)} \end{array}\right] \tag{13}$$

Before integrating $\int\int_{\partial SO} dS$ over the spheroidal surface, where

$$dS = f^2\left(\xi^2 - 1\right)^{\frac{1}{2}} d\phi d\eta \left(\xi^2 - \eta^2\right)^{\frac{1}{2}} \tag{14}$$

where the function $f = d/2$ and d is the interfocal distance.

We multiply by a $g^{Me}(\eta)$ function in the dot product. This is introduced to avoid singularity in the integration. In this paper, we choose

$$g^{Me}(\eta) = g^{Mo}(\eta) = g^{Ne}(\eta) = g^{No}(\eta) = g(\eta) = \left(1 - \eta^2\right)\left(\xi^2 - \eta^2\right)^3 \tag{15}$$

Thus to illustrate one such integration for a term on the right hand side of Equation (13), using

$$\bar{M}^{a(i)}_{(e,o)mn} = M^{a(i)}_{(e,o)m,n,\eta}\hat{\eta} + M^{a(i)}_{(e,o)m,n,\xi}\hat{\xi} + M^{a(i)}_{(e,o)m,n,\phi}\hat{\phi} \tag{16}$$

we define

$$\begin{aligned} C^{M,e,M,o}_{m'n'mn} =& \int_{\partial SO} dS\hat{\xi} \times \bar{M}^{a(3)}_{o,mn} \cdot \bar{M}^{a(3)}_{e,m'n'} g^{Me}(\eta) \\ =& f^2\left(\xi^2-1\right)^{\frac{1}{2}} \int_0^{2\pi} d\phi \int_{-1}^{1} d\eta \left\{ \left(\xi^2-\eta^2\right)^{\frac{1}{2}} g^{Me}(\eta) \times \left[-M^{a(3)}_{o,mn\eta} M^{a(3)}_{e,m'n'\phi} + M^{a(3)}_{o,mn\phi} M^{a(3)}_{e,m'n'\eta} \right] \right\} \end{aligned} \tag{17}$$

We next use

$$\begin{aligned} &M^{a(3)}_{e,mn\eta} = f^{M\eta}_{mn}(\eta)\sin(m\phi); M^{a(3)}_{o,mn\eta} = -f^{M\eta}_{mn}(\eta)\cos(m\phi); \\ &M^{a(3)}_{e,mn\phi} = f^{M\phi}_{mn}(\eta)\cos(m\phi); M^{a(3)}_{o,mn\phi} = f^{M\phi}_{mn}(\eta)\sin(m\phi). \end{aligned} \tag{18}$$

where the f s are given in the appendix.

The integration $\int_0^{2\pi} d\phi$ is just over products of $\sin(m\phi)$ and $\cos(m\phi)$.

We then have

$$C^{M,e,M,o}_{m'n'mn} = \pi\delta_{mm'} f^2\left(\xi^2-1\right)^{\frac{1}{2}} \int_{-1}^{1} d\eta \left\{ \left(\xi^2-\eta^2\right)^{\frac{1}{2}} g^{Me}(\eta) \left[f^{M\eta}_{mn}(\eta) f^{M\phi}_{m'n'}(\eta) + f^{M\phi}_{mn}(\eta) f^{M\eta}_{m'n'}(\eta) \right] \right\} \tag{19}$$

This integration will be examined later. It is noted that the case when $m = m' = 0$ is excluded here.

Because we have 4 terms on the right side of Equation (13), there are in total 16 coefficients of $C's$. Beside the $C^{M,e,M,o}_{m'n'mn}$, the rest of the 15 coefficients are listed below.

$$C^{M,e,M,e}_{mnm'n'} = 0 \tag{20}$$

$$C^{M,e,N,e}_{m'n'mn} = \pi\delta_{mm'} f^2\left(\xi^2-1\right)^{\frac{1}{2}} \int_{-1}^{1} d\eta \left\{ \left(\xi^2-\eta^2\right)^{\frac{1}{2}} g^{Me}(\eta) \left[-f^{N\eta}_{mn}(\eta) f^{M\phi}_{m'n'}(\eta) + f^{N\phi}_{mn}(\eta) f^{M\eta}_{m'n'}(\eta) \right] \right\} \tag{21}$$

$$C^{M,e,N,o}_{mnm'n'} = 0 \tag{22}$$

Using g^{Mo}, we have

$$\begin{aligned} C^{M,o,M,e}_{m'n'mn} =& \int_{\partial SO} \hat{\xi} \times \bar{M}^{a(3)}_{e,mn} \cdot \bar{M}^{a(3)}_{o,m'n'} g^{Mo}(\eta) \\ =& \pi\delta_{mm'} f^2\left(\xi^2-1\right)^{\frac{1}{2}} \int_{-1}^{1} d\eta \left\{ \left(\xi^2-\eta^2\right)^{\frac{1}{2}} g^{Mo}(\eta) \left[-f^{M\eta}_{mn}(\eta) f^{M\phi}_{m'n'}(\eta) - f^{M\phi}_{mn}(\eta) f^{M\eta}_{m'n'}(\eta) \right] \right\} \end{aligned} \tag{23}$$

$$C^{M,o,M,o}_{m'n'mn} = \int_{\partial SO} \hat{\xi} \times \bar{M}^{a(3)}_{o,mn} \cdot \bar{M}^{a(3)}_{o,m'n'} g^{Mo}(\eta) = 0 \tag{24}$$

$$C^{M,o,N,e}_{m'n'mn} = \int_{\partial SO} \hat{\xi} \times \bar{N}^{a(3)}_{e,mn} \cdot \bar{M}^{a(3)}_{o,m'n'} g^{Mo}(\eta) = 0 \tag{25}$$

$$\begin{aligned} C^{M,o,N,o}_{m'n'mn} =& \int_{\partial SO} \hat{\xi} \times \bar{N}^{a(3)}_{o,mn} \cdot \bar{M}^{a(3)}_{o,m'n'} g^{Mo}(\eta) \\ =& \pi\delta_{mm'} f^2\left(\xi^2-1\right)^{\frac{1}{2}} \int_{-1}^{1} d\eta \left\{ \left(\xi^2-\eta^2\right)^{\frac{1}{2}} g^{Mo}(\eta) \left[-f^{N\eta}_{mn}(\eta) f^{M\phi}_{m'n'}(\eta) + f^{N\phi}_{mn}(\eta) f^{M\eta}_{m'n'}(\eta) \right] \right\} \end{aligned} \tag{26}$$

Using g^{Ne}. Similarly, we obtain

$$\begin{aligned} C^{N,e,M,e}_{m'n'mn} =& \int_{\partial SO} \hat{\xi} \times \bar{M}^{a(3)}_{e,mn} \cdot \bar{N}^{a(3)}_{e,m'n'} g^{Ne}(\eta) \\ =& \pi\delta_{mm'} f^2\left(\xi^2-1\right)^{\frac{1}{2}} \int_{-1}^{1} d\eta \left\{ \left(\xi^2-\eta^2\right)^{\frac{1}{2}} g^{Ne}(\eta) \left[-f^{M\eta}_{mn}(\eta) f^{N\phi}_{m'n'}(\eta) + f^{M\phi}_{mn}(\eta) f^{N\eta}_{m'n'}(\eta) \right] \right\} \end{aligned} \tag{27}$$

$$C^{N,e,M,o}_{m'n'mn} = \int_{\partial SO} \hat{\xi} \times \bar{M}^{a(3)}_{o,mn} \cdot \bar{N}^{a(3)}_{e,m'n'} g^{Ne}(\eta) = 0 \tag{28}$$

$$C^{N,e,N,e}_{m'n'mn} = \int_{\partial SO} \hat{\xi} \times \bar{N}^{a(3)}_{e,mn} \cdot \bar{N}^{a(3)}_{e,m'n'} g^{Ne}(\eta) = 0 \tag{29}$$

$$\begin{aligned} C^{N,e,N,o}_{m'n'mn} &= \int_{\partial SO} \hat{\xi} \times \bar{N}^{a(3)}_{o,mn} \cdot \bar{N}^{a(3)}_{e,m'n'} g^{Ne}(\eta) \\ &= \pi\delta_{mm'} f^2\left(\xi^2-1\right)^{\frac{1}{2}} \int_{-1}^{1} d\eta \left\{ \left(\xi^2-\eta^2\right)^{\frac{1}{2}} g^{Ne}(\eta) \left[-f^{N\eta}_{mn}(\eta) f^{N\phi}_{m'n'}(\eta) - f^{N\phi}_{mn}(\eta) f^{N\eta}_{m'n'}(\eta) \right] \right\} \end{aligned} \tag{30}$$

Using g^{No}. Similarly, we obtain

$$C^{N,o,M,e}_{m'n'mn} = \int_{\partial SO} \hat{\xi} \times \bar{M}^{a(3)}_{e,mn} \cdot \bar{N}^{a(3)}_{o,m'n'} g^{No}(\eta) = 0 \tag{31}$$

$$\begin{aligned} C^{N,o,M,o}_{m'n'mn} &= \int_{\partial SO} \hat{\xi} \times \bar{M}^{a(3)}_{o,mn} \cdot \bar{N}^{a(3)}_{o,m'n'} g^{No}(\eta) \\ &= \pi\delta_{mm'} f^2\left(\xi^2-1\right)^{\frac{1}{2}} \int_{-1}^{1} d\eta \left\{ \left(\xi^2-\eta^2\right)^{\frac{1}{2}} g^{No}(\eta) \left[-f^{M\eta}_{mn}(\eta) f^{N\phi}_{m'n'}(\eta) + f^{M\phi}_{mn}(\eta) f^{N\eta}_{m'n'}(\eta) \right] \right\} \end{aligned} \tag{32}$$

$$\begin{aligned} C^{N,o,N,e}_{m'n'mn} &= \int_{\partial SO} \hat{\xi} \times \bar{N}^{a(3)}_{e,mn} \cdot \bar{N}^{a(3)}_{o,m'n'} g^{No}(\eta) \\ &= \pi\delta_{mm'} f^2\left(\xi^2-1\right)^{\frac{1}{2}} \int_{-1}^{1} d\eta \left\{ \left(\xi^2-\eta^2\right)^{\frac{1}{2}} g^{No}(\eta) \left[f^{N\eta}_{mn}(\eta) f^{N\phi}_{m'n'}(\eta) + f^{N\phi}_{mn}(\eta) f^{N\eta}_{m'n'}(\eta) \right] \right\} \end{aligned} \tag{33}$$

$$C^{N,o,N,o}_{m'n'mn} = \int_{\partial SO} \hat{\xi} \times \bar{N}^{a(3)}_{o,mn} \cdot \bar{N}^{a(3)}_{o,m'n'} g^{No}(\eta) = 0 \tag{34}$$

The next step is to calculate the integrations over η. Following is a summary of the integration needed to be computed.

$$\begin{aligned} &\int_{-1}^{1} d\eta \left(\xi^2-\eta^2\right)^{\frac{1}{2}} f^{M\eta}_{mn}(\eta)\, f^{M\phi}_{m'n'}(\eta)\, g(\eta)\,; \int_{-1}^{1} d\eta \left(\xi^2-\eta^2\right)^{\frac{1}{2}} f^{N\eta}_{mn}(\eta)\, f^{M\phi}_{m'n'}(\eta)\, g(\eta) \\ &\int_{-1}^{1} d\eta \left(\xi^2-\eta^2\right)^{\frac{1}{2}} f^{N\phi}_{mn}(\eta)\, f^{M\eta}_{m'n'}(\eta)\, g(\eta)\,; \int_{-1}^{1} d\eta \left(\xi^2-\eta^2\right)^{\frac{1}{2}} f^{N\phi}_{mn}(\eta)\, f^{N\eta}_{m'n'}(\eta)\, g(\eta) \end{aligned} \tag{35}$$

$f(\eta)$s are singular as shown in Appendix A. The product with $g(\eta)$ removes the singularities. For example, the integrand $\left(\xi^2-\eta^2\right)^{\frac{1}{2}} f^{N\phi}_{mn}(\eta)\, f^{N\eta}_{m'n'}(\eta)\, g(\eta)$ is also plotted in Fig. 3, which shows no singularity over the range of η.

Then, these functions are ready to be integrated numerically to find the matrix $\bar{\bar{C}}$.

Next, we consider calculations of the left hand side of Equation (13)

$$b^{Me}_{m'n'} = \int_{\partial SO} dS g^{Me}(\eta)\, \widehat{\xi} \times \bar{E}^s \cdot \bar{M}^{a(3)}_{e,m'n'} \tag{36}$$

$$= f^2\left(\xi^2-1\right)^{\frac{1}{2}} \int_0^{2\pi} d\phi \int_{-1}^{1} d\eta \left(\xi^2-\eta^2\right)^{\frac{1}{2}} g^{Me}(\eta)\, \widehat{\xi} \times \bar{E}^s \cdot \bar{M}^{a(3)}_{e,m'n'} \tag{37}$$

Since $\bar{E}^s$ is calculated numerically by HFSS, the Equation (37) is a 2 dimensional integration over ϕ and η.

The other 3 terms are

$$b^{Mo}_{m'n'} = \int_{\partial SO} dS g^{Me}(\eta)\, \widehat{\xi} \times \bar{E}^s \cdot \bar{M}^{a(3)}_{o,m'n'} \tag{38}$$

$$b^{Ne}_{m'n'} = \int_{\partial SO} dS g^{Me}(\eta)\, \widehat{\xi} \times \bar{E}^s \cdot \bar{N}^{a(3)}_{e,m'n'} \tag{39}$$

$$b^{No}_{m'n'} = \int_{\partial SO} dS g^{Me}(\eta)\, \widehat{\xi} \times \bar{E}^s \cdot \bar{N}^{a(3)}_{o,m'n'} \tag{40}$$

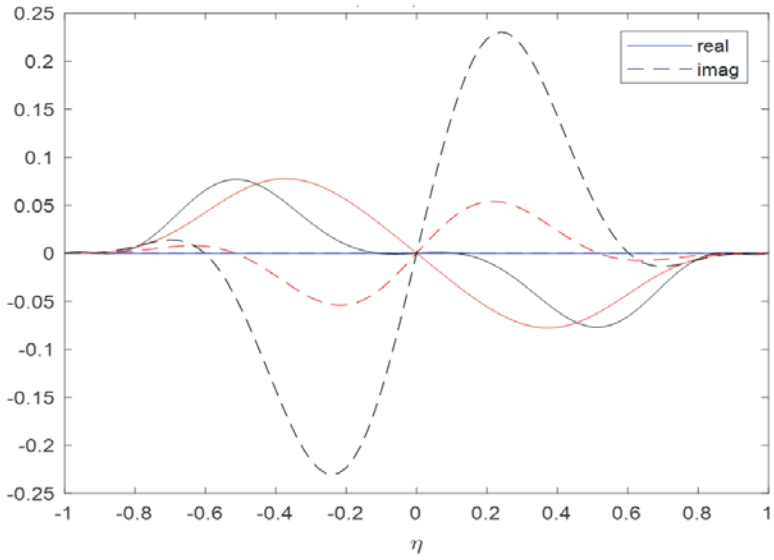

Figure 3. Plot of the integrand in Equation (35) at $c = 3.8773, \xi = 1.05, (m', n') = (m, n)$; blue: $(m, n) = (0, 1)$, red: $(m, n) = (1, 1)$, and black: $(m, n) = (1, 2)$.

We use HFSS to calculate $\bar{E}^s$. In HFSS, the output scattered fields are usually defined in the rectangular coordinates $\bar{E} = E_x\hat{x} + E_y\hat{y} + E_z\hat{z}$. Thus, the output scattered fields need to be transformed into spheroidal coordinates $\bar{E} = E_\eta\hat{\eta} + E_\xi\hat{\xi} + E_\phi\hat{\phi}$. Using the $\hat{\eta}$, $\hat{\xi}$ and $\hat{\phi}$ unit vector in terms of Cartesian unit vector, we obtain

$$E_\eta = -\eta\frac{\left(\xi^2-1\right)^{\frac{1}{2}}}{\left(\xi^2-\eta^2\right)^{\frac{1}{2}}}\left(E_x\cos\phi + E_y\sin\phi\right) + \xi\frac{\left(1-\eta^2\right)^{\frac{1}{2}}}{\left(\xi^2-\eta^2\right)^{\frac{1}{2}}}E_z \tag{41}$$

$$E_\xi = \xi\frac{\left(1-\eta^2\right)^{\frac{1}{2}}}{\left(\xi^2-\eta^2\right)^{\frac{1}{2}}}\left(E_x\cos\phi + E_y\sin\phi\right) + E_z\frac{\left(\xi^2-1\right)^{\frac{1}{2}}}{\left(\xi^2-\eta^2\right)^{\frac{1}{2}}}\hat{z} \tag{42}$$

$$E_\phi = -E_x\sin\phi + E_y\cos\phi \tag{43}$$

2.4.2. Matrix Notations

The matrix notation for spherical waves is detailed in [1]. In using spheroidal waves, we consider prolate spheroids of relatively moderate to large aspect ratio because that resemble the branching structure of vegetation. If the aspect ratio is comparable to 1, then we can just use spherical waves. Thus we are considering cases with aspect ratio of 3 to 20 times. In this case, we use separate $M_{\max}$ and $N_{\max}$. Thus the counting is

$$\begin{aligned} &m = 0, \\ &n = 1, 2, \ldots N_{\max}; \\ &m = 1, \\ &n = 1, 2, \ldots N_{\max}; \\ &\ldots \\ &m = M_{\max}, \\ &n = 1, 2, \ldots N_{\max}. \end{aligned} \tag{44}$$

Then, the total number of terms is

$$(M_{\max} + 1)N_{\max} = L_{\max} \tag{45}$$

Suppose $N_{\max} = 5$, $M_{\max} = 1$, the values of m, n, and l are listed below.

$$\begin{array}{cccccccccccc} n & 1 & 2 & 3 & 4 & 5 & 1 & 2 & 3 & \ldots & 4 & 5 \\ m & 0 & 0 & 0 & 0 & 0 & 0 & 1 & 1 & \ldots & 1 & 1 \\ l & 1 & 2 & 3 & 4 & 5 & 6 & 7 & 8 & \ldots & 9 & 10 \end{array} \tag{46}$$

The dimension is

$$(M_{\max} + 1)N_{\max} = 2 \times 5 = 10 \tag{47}$$

In matrix notations,

$$\begin{bmatrix} \bar{b}^{M,e} \\ \bar{b}^{M,o} \\ \bar{b}^{N,e} \\ \bar{b}^{N,o} \end{bmatrix} = \begin{bmatrix} \bar{\bar{C}}^{M,e,M,e} & \bar{\bar{C}}^{M,e,M,o} & \bar{\bar{C}}^{M,e,N,e} & \bar{\bar{C}}^{M,e,N,o} \\ \bar{\bar{C}}^{M,o,M,e} & \bar{\bar{C}}^{M,o,M,o} & \bar{\bar{C}}^{M,o,N,e} & \bar{\bar{C}}^{M,o,N,o} \\ \bar{\bar{C}}^{N,e,M,e} & \bar{\bar{C}}^{N,e,M,o} & \bar{\bar{C}}^{N,e,N,e} & \bar{\bar{C}}^{N,e,N,o} \\ \bar{\bar{C}}^{N,o,M,e} & \bar{\bar{C}}^{N,o,M,o} & \bar{\bar{C}}^{N,o,N,e} & \bar{\bar{C}}^{N,o,N,o} \end{bmatrix} \begin{bmatrix} \bar{a}^{S(M),e} \\ \bar{a}^{S(M),o} \\ \bar{a}^{S(N),e} \\ \bar{a}^{S(N),o} \end{bmatrix} \tag{48}$$

$$\begin{aligned} \bar{b}^{Me} &= \text{dimension of } L_{\max} \times 1 \\ \bar{a}^{S(M),e} &= \text{dimension of } L_{\max} \times 1 \\ \bar{\bar{C}}^{M,e,M,e} &= \text{dimension of } L_{\max} \times L_{\max} \end{aligned}$$

Then, in more compact notations,

$$\begin{bmatrix} \bar{b}^{(M)} \\ \bar{b}^{(N)} \end{bmatrix} = \begin{bmatrix} \bar{\bar{C}}^{(M)(M)} & \bar{\bar{C}}^{(M)(N)} \\ \bar{\bar{C}}^{(N)(M)} & \bar{\bar{C}}^{(N)(N)} \end{bmatrix} \begin{bmatrix} \bar{a}^{S(M)} \\ \bar{a}^{S(N)} \end{bmatrix} \tag{49}$$

where

$$\begin{aligned} \bar{b}^{M} &= \begin{bmatrix} \bar{b}^{M,e} \\ \bar{b}^{M,o} \end{bmatrix} \\ \bar{b}^{(N)} &= \begin{bmatrix} \bar{b}^{N,e} \\ \bar{b}^{N,o} \end{bmatrix} \end{aligned}$$

Then, the scattered field coefficients are obtained as

$$\begin{bmatrix} \bar{a}^{S(M)} \\ \bar{a}^{S(N)} \end{bmatrix} = \begin{bmatrix} \bar{\bar{C}}^{(M)(M)} & \bar{\bar{C}}^{(M)(N)} \\ \bar{\bar{C}}^{(N)(M)} & \bar{\bar{C}}^{(N)(N)} \end{bmatrix}^{-1} \begin{bmatrix} \bar{b}^{(M)} \\ \bar{b}^{(N)} \end{bmatrix} \tag{50}$$

2.4.3. Calculations of $\bar{a}_l^E$ for Vector Spheroidal Waves

To obtain the T-matrix, we next compute the exciting field coefficients. The T-matrix is of dimension $4L_{\max} \times 4L_{\max}$. Thus, we choose $4L_{\max}$ incident plane waves, which includes the 2 incident polarizations of TE and TM. Then, the number of angles are $2L_{\max}$, chosen over (θ_i, ϕ_i).

The incident plane waves are expanded in terms of incoming prolate spheroidal waves [32]. For TE plane wave,

$$\bar{E}^{\text{plane,TE}} = \sum_{n=1}^{N_{\max}} \sum_{m=0}^{n} i^n \left[f_{mn}^{(2)} \bar{M}_{e,Mn}^{r(1)} + i f_{mn}^{(1)} \bar{N}_{o,mn}^{r(1)} \right] \tag{51}$$

For TM plane wave,

$$\bar{E}^{\text{plane,TM}} = \sum_{n=1}^{N_{\max}} \sum_{m=0}^{n} i^n \left[f_{mn}^{(1)} \bar{M}_{o,mn}^{r(1)} - i f_{mn}^{(2)} \bar{N}_{e,mn}^{r(1)} \right] \tag{52}$$

where

$$f_{mn}^{(1)}(\theta_i) = \frac{4m}{\Lambda_{mn}} \sum_{r=0,1}^{\infty'} \frac{d_r^{mn}}{(r+m)(r+m+1)} \frac{P_{m+r}^m(\cos\theta_i)}{\sin\theta_i} \tag{53}$$

$$f_{mn}^{(2)}(\theta_i) = \frac{2\,(2-\delta_{0m})}{\Lambda_{mn}} \sum_{r=0,1}^{\infty'} \frac{d_r^{mn}}{(r+m)(r+m+1)} \frac{dP_{m+r}^m(\cos\theta_i)}{d\theta_i} \tag{54}$$

d_r^{mn} is the coefficients in calculating the spheroidal wave functions as explained in Appendix A. The definition of Λ_{mn} is

$$\Lambda_{mn} = \sum_{r=0,1}^{\infty'} \frac{(|m|+M+r)!}{(|m|-m+r)!} \frac{2}{2(|m|+r)+1} d_r^{mn*}(c) d_r^{mn}(c) \tag{55}$$

The incident plane waves propagate in the xz plane at angle θ_i to the z axis.

Then,

$$\begin{aligned} \bar{a}_{mn}^{E(M)} &= i^n f_{mn}^{(2)}, \bar{a}_1^{E(N)} = i^{n+1} f_{mn}^{(1)}, \text{ for TE waves} \\ \bar{a}_{mn}^{E(M)} &= i^n f_{mn}^{(1)}, \bar{a}_1^{E(N)} = -i^{n+1} f_{mn}^{(2)}, \text{ for TM waves} \end{aligned} \tag{56}$$

The superscript '(1)' is used in $\bar{M}_{mn}^{r(1)}$, $\bar{N}_{mn}^{r(1)}$ because the incident waves are expanded in terms of income vector spheroidal waves.

For each incident plane wave, we compute

$$\begin{bmatrix} \bar{a}^{E(M)} \\ \bar{a}^{E(N)} \end{bmatrix}$$

We also compute the scattered near field using on the spheroidal surface $\bar{E}^{(S)}$ from HFSS and, then calculate

$$\begin{bmatrix} \bar{a}^{S(M)} \\ \bar{a}^{S(N)} \end{bmatrix}$$

After the expansion coefficients for both scattered fields and the corresponding incident fields are computed, the T-matrix with vector spheroidal waves is obtained for irregular objects.

3. NUMERICAL ILLUSTRATIONS OF T-MATRIX EXTRACTIONS AND VALIDATIONS

To validate the T-matrix of complex object, we validate using the following methodology.

Figure 4 shows a complex object of a branch with leaves attached. The results of the scattered field are computed in 2 ways. The first method is the direct method using HFSS to calculate the far

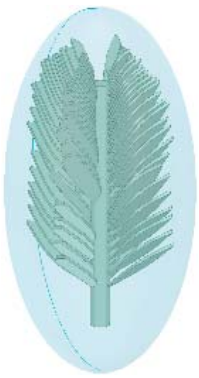

Figure 4. A branch with leaves attached for T-matrix validation.

field bistatic cross sections. The results of this method are the benchmark solutions. In the second method, we use the near fields scattered fields of HFSS to extract the T-matrix of vector spheroidal waves. Then, we use the extracted T-matrix to calculate the scattered far fields using the far field solutions of vector spheroidal waves. By showing that the results of method 2 and method 1 agree, the extraction of T-matrix for complex objects using spheroidal waves are validated.

To illustrate method 2, consider plane wave incidence, the exciting field coefficients are as before. Using the extracted T-matrix, the expansion coefficients $\bar{a}^S$ of the scattered waves are obtained

$$\bar{a}^S = \bar{\bar{T}}\bar{a}^E \tag{57}$$

Then, the scattered fields are

$$\bar{E}^s = \sum_{n=1}^{N\max}\sum_{m=0}^{n}\left[a_{mn}^{S(M),e}\bar{M}_{e,mn}^{a(3)} + a_{mn}^{S(N),e}\bar{N}_{e,mn}^{a(3)}\right] + \sum_{n=1}^{N\max}\sum_{m=1}^{n}\left[a_{mn}^{S(M),o}\bar{M}_{o,mn}^{a(3)} + a_{mn}^{S(N),o}\bar{N}_{o,mn}^{a(3)}\right] \tag{58}$$

Note that the difference between as here and the $\bar{a}^S$ before is: the $\bar{a}^S$ before in equations are calculated using the near fields of HFSS. They are then used to obtain the T-matrix, while the $\bar{a}^S$ here are calculated from the T-matrix.

The asymptotic forms of $\bar{M}_{(e,o),mn}^{r(3)}$ and $\bar{N}_{(e,o),mn}^{r(3)}$ are [40]

$$M_{(e,o),m,n,\eta}^{r(3)} \to (-i)^{n+1}\frac{mS_{mn}(\cos\theta)}{\sin\theta}\frac{\exp(ikr)}{kr}\begin{bmatrix}\sin(m\phi)\\ -\cos(m\phi)\end{bmatrix} \tag{59}$$

$$M_{(e,o),m,n,\phi}^{r(3)} \to -(-i)^{n+1}\frac{dS_{mn}(\cos\theta)}{d\theta}\frac{\exp(ikr)}{kr}\begin{bmatrix}\cos(m\phi)\\ \sin(m\phi)\end{bmatrix} \tag{60}$$

$$N_{(e,o),m,n,\eta}^{r(3)} \to -(-i)^{n}\frac{dS_{mn}(\cos\theta)}{d\theta}\frac{\exp(ikr)}{kr}\begin{bmatrix}\cos(m\phi)\\ \sin(m\phi)\end{bmatrix} \tag{61}$$

$$N_{(e,o),m,n,\phi}^{r(3)} \to -(-i)^{n}\frac{mS_{mn}(\cos\theta)}{\sin\theta}\frac{\exp(ikr)}{kr}\begin{bmatrix}\sin(m\phi)\\ -\cos(m\phi)\end{bmatrix} \tag{62}$$

Thus, in the far field region,

$$E_{s,\eta} = \frac{\exp(ikr)}{kr}\sum_{m,n}\begin{bmatrix}\left(a_{mn}^{S(M)e}\sin(m\phi) - a_{mn}^{S(M)o}\cos(m\phi)\right)\dfrac{(-i)^{n+1}mS_{mn}(\cos\theta)}{\sin\theta}\\ -\left(a_{mn}^{S(N)e}\cos(m\phi) + a_{mn}^{S(N)o}\sin(m\phi)\right)\dfrac{(-i)^{n}dS_{mn}(\cos\theta)}{d\theta}\end{bmatrix} \tag{63}$$

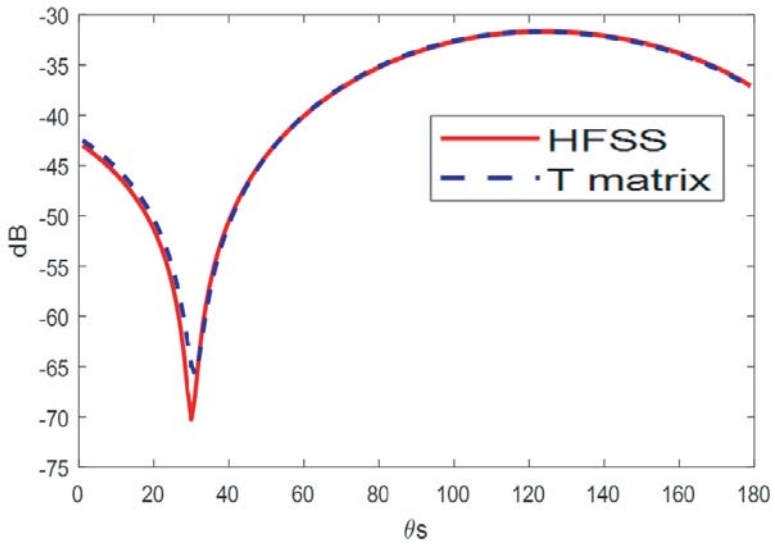

Figure 5. σ_{vv} from HFSS (method 1) compared with that from the T-matrix (method 2).

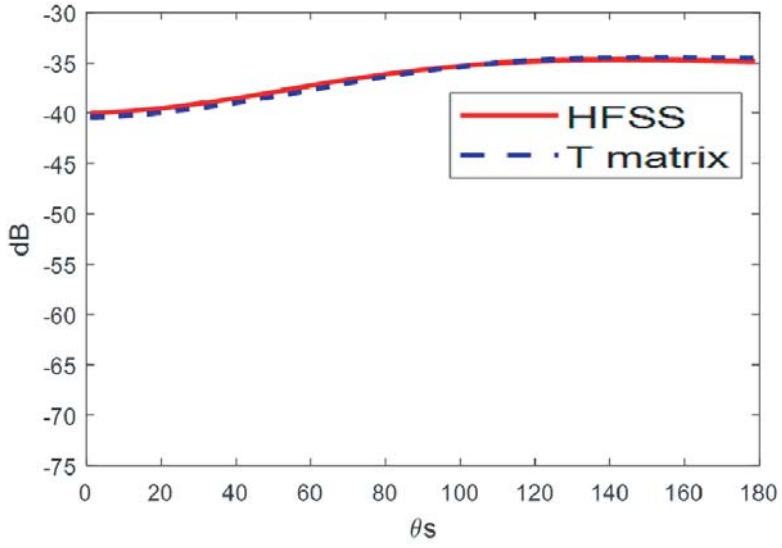

Figure 6. σ_{hh} from HFSS (method 1) compared with that from the T-matrix (method 2).

$$E_{s,\phi} = \frac{\exp(ikr)}{kr} \sum_{m,n} \begin{bmatrix} \left(a_{mn}^{S(M)e} \cos(m\phi) + a_{mn}^{S(M)o} \sin(m\phi)\right) \dfrac{-(-i)^{n+1} dS_{mn}(\cos\theta)}{d\theta} \\ -\left(a_{mn}^{S(N)e} \sin(m\phi) - a_{mn}^{S(N)o} \cos(m\phi)\right) \dfrac{(-i)^n m S_{mn}(\cos\theta)}{\sin\theta} \end{bmatrix} \tag{64}$$

Finally, using the relationship that $\begin{bmatrix} E_v^s \\ E_h^s \end{bmatrix} = \frac{\exp(ikr)}{r} \begin{bmatrix} S_{vv} & S_{vh} \\ S_{hv} & S_{hh} \end{bmatrix} \begin{bmatrix} E_v^i \\ E_h^i \end{bmatrix}$ and $\sigma_{pq} = 4\pi |S_{pq}|^2$, the radar cross section (RCS) of the scatterer using the T-matrix of method 2 is obtained.

The RCS are computed using two methods for a branch with complicated leaves (Fig. 4). The results are shown in Fig. 5 and Fig. 6. The length of the center stalk of the branch is $8cm$ and the permittivity is $27.22 + 5.22i$ with frequency at $1.41GHz$. The T-matrix is extracted from HFSS using the method in section 2. It can be seen that the results from the T-matrix and HFSS are in good agreement This good agreement verifies the correctness of the T-matrix with vector spheroidal wave expansions.

4. NUMERICAL TRANSLATION ADDITION THEOREM FOR VECTOR SPHEROIDAL WAVES

Consider two spheroids (e.g., Fig. 2(b)), one centered at $\bar{r}_l$ and the other centered at $\bar{r}_j$. Consider an outgoing spheroidal wave $\bar{M}_{\sigma,mn}^{a(3)}(c, \xi_j, \eta_j, \phi_j)$ from spheroid j. The translation addition theorem says that the outgoing waves can be expressed as a linear combination of incoming waves on particle l (Fig. 7).

The mathematical expressions for the translation addition theorem for vector spheroidal waves are [1]

$$\bar{M}_{\sigma',\mu'\nu'}^{a(3)}(c, \xi_j, \eta_j, \phi_j) = \sum_{\sigma,\mu,\nu} \left[\bar{M}_{\sigma,\mu\nu}^{a(1)}(kr\bar{r}_l) A_{M\sigma\mu\nu,M\sigma'\mu'\nu'} + \bar{N}_{\sigma,\mu\nu}^{a(1)}(kr\bar{r}_l) A_{N\sigma\mu\nu,M\sigma'\mu'\nu'}\right] \tag{65}$$

Taking $\nabla\times$ on both sides of the above equation and using the properties that $\nabla \times \bar{M} = k\bar{N}$ and $\nabla \times \bar{N} = k\bar{M}$, we have

$$\bar{N}_{\sigma',\mu'\nu'}^{a(3)}(c, \xi_j, \eta_j, \phi_j) = \sum_{\sigma,\mu,\nu} \left[\bar{M}_{\sigma,\mu\nu}^{a(1)}(kr\bar{r}_l) A_{N\sigma\mu\nu,M\sigma'\mu'\nu'} + \bar{N}_{\sigma,\mu\nu}^{a(1)}(kr\bar{r}_l) A_{M\sigma\mu\nu,M\sigma'\mu'\nu'}\right] \tag{66}$$

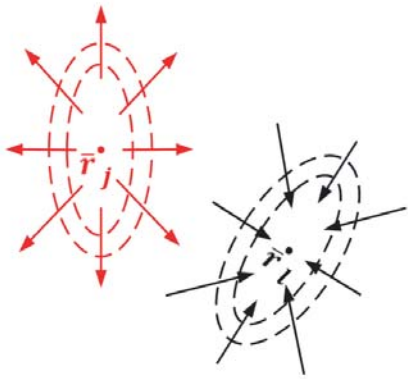

Figure 7. Illustration of translation addition theorem of vector spheroidal waves: outgoing spheroidal waves centered at $\bar{r}_j$ are transformed to incoming spheroidal waves centered at $\bar{r}_l$.

where σ is either 'e' or 'o'. These equations mean the outgoing vector spheroidal waves $\bar{M}^{a(3)}_{\sigma,mn}(c,\xi_j,\eta_j,\phi_j)$ and $\bar{N}^{a(3)}_{\sigma,mn}(c,\xi_j,\eta_j,\phi_j)$ centered at $\bar{r}_j$ are expressed the incoming vector spheroidal waves $\bar{M}^{a(1)}_{\sigma,\mu\nu}(kr\bar{r}_l)$ and $\bar{N}^{a(1)}_{\sigma,\mu\nu}(kr\bar{r}_l)$ centered at $\bar{r}_l$. $A_{M\sigma\mu\nu,M\sigma'\mu'\nu'}$ and $A_{N\sigma\mu\nu,M\sigma'\mu'\nu'}$ are the transformation coefficients. We only need the $\bar{M}^{a(3)}_{\sigma',\mu'\nu'}(c,\xi_j,\eta_j,\phi_j)$ (i.e., Equation (65)) to derive the translational addition coefficients since the $\bar{N}^{a(3)}_{\sigma',\mu'\nu'}(c,\xi_j,\eta_j,\phi_j)$ follows from it.

For vector spheroidal waves, unlike spherical waves, we do not need to have $\mu = 0,1,2,\ldots,\nu$ because we are using prolate spheroidal waves for moderate to large aspect ratio. Thus, in this case, we use separate $M_{\max}$ and $N_{\max}$. The number of μ and ν combinations is $L_{\max} = (M_{\max}+1)N_{\max}$. To count the number of coefficients, we combine the two indices, and write $(\mu,\nu),(m,n)$ etc. as $1,2,\ldots L_{\max}$. Thus for (μ,ν) and (μ',ν') which are independent inside the summation in Equation (65), we have $L^2_{\max}$. In addition, there is a factor of 2 for"even" and "odd" for σ. Thus for σ and σ' which are independent, we have 4 combinations. However, for 2 polarizations, $\bar{M}$ and $\bar{N}$, the count needs to be careful because the two equation above are the same. Thus, we only have M,M and N,M, in the subscripts of A and not M,N nor N,N. Thus, the count is only 2 and not 4. For the combined index of (σ,μ,ν), there are $2L_{\max}$ indices. There are $4L^2_{\max}$ indices in each of $A_{M\sigma\mu\nu,M\sigma'\mu'\nu'}$ and $A_{N\sigma\mu\nu,M\sigma'\mu'\nu'}$. Because the factor is only 2 for polarization combinations, the total number of the translation addition coefficients to be determined in $A_{M\sigma\mu\nu,M\sigma'\mu'\nu'}$ and $A_{N\sigma\mu\nu,M\sigma'\mu'\nu'}$ is $8L^2_{\max}$.

Following is the summary of the steps to obtain the coefficients A.

Step (1): take cross product of Equation (65) with the normal $\hat{\xi}_{\bar{r}_l}$ of spheroidal l.

Let $\sigma' = e$. We have the equation

$$\hat{\xi}_{\bar{r}_l}\times\bar{M}^{a(3)}_{e,\mu'\nu'}(c,\xi_j,\eta_j,\phi_j) = \sum_{\mu,\nu}\left[\begin{array}{l}\hat{\xi}_{\bar{r}_l}\times\bar{M}^{a(1)}_{e,\mu\nu}(kr\bar{r}_l)\,A_{Me\mu\nu,Me\mu'\nu'}+\hat{\xi}_{\bar{r}_l}\times\bar{M}^{a(1)}_{o,\mu\nu}(kr\bar{r}_l)\,A_{Mo\mu\nu,Me\mu'\nu'}\\ +\hat{\xi}_{\bar{r}_l}\times\bar{N}^{a(1)}_{e,\mu\nu}(kr\bar{r}_l)\,A_{Ne\mu\nu,Me\mu'\nu'}\ +\hat{\xi}_{\bar{r}_l}\times\bar{N}^{a(1)}_{o,\mu\nu}(kr\bar{r}_l)\,A_{No\mu\nu,Me\mu'\nu'}\end{array}\right] \quad (67)$$

Let $\sigma' = o$,

$$\hat{\xi}_{\bar{r}_l}\times\bar{M}^{a(3)}_{o,\mu'\nu'}(c,\xi_j,\eta_j,\phi_j) = \sum_{\mu,\nu}\left[\begin{array}{l}\hat{\xi}_{\bar{r}_l}\times\bar{M}^{a(1)}_{e,\mu\nu}(kr\bar{r}_l)\,A_{Me\mu\nu,Mo\mu'\nu'}+\hat{\xi}_{\bar{r}_l}\times\bar{M}^{a(1)}_{o,\mu\nu}(kr\bar{r}_l)\,A_{Mo\mu\nu,Mo\mu'\nu'}\\ +\hat{\xi}_{\bar{r}_l}\times\bar{N}^{a(1)}_{e,\mu\nu}(kr\bar{r}_l)\,A_{Ne\mu\nu,Mo\mu'\nu'}\ +\hat{\xi}_{\bar{r}_l}\times\bar{N}^{a(1)}_{o,\mu\nu}(kr\bar{r}_l)\,A_{No\mu\nu,Mo,\mu'\nu'}\end{array}\right] \quad (68)$$

Note that there are changes between Left-Hand-Side (LHS) of Equations (67) and (68). Between the Righ-Hand-Side (RHS) of Equations (67) and (68), only the $A's$ coefficients change because σ' is changed. The cross products remain the same on the RHS. Both Equations (67) and (68) have 4 terms under the summation sign. Let $(\mu,\nu) = 1,\ldots L_{\max}$ and $(\mu',\nu') = 1,\ldots L_{\max}$, then Equation (67) has $4L^2_{\max}$ coefficients of $A's$ and Equation (68) also has $4L^2_{\max}$ coefficients of $A's$, giving a total of $8L^2_{\max}$ coefficients of $A's$.

Step (2): Use Equation (67) which has $\sigma' = e$. Take the dot product of Equation (67) 'in front' with $\bar{M}^{a(1)}_{e,mn}(kr\bar{r}_l)$ and integration over the surface of spheroidal l.

$$\begin{aligned}
&\int_{\partial SO_l} dS\bar{M}^{a(1)}_{e,mn}(kr\bar{r}_l)\cdot\hat{\xi}_{\bar{r}_l}\times\bar{M}^{a(3)}_{e,\mu'\nu'}(c,\xi_j,\eta_j,\phi_j) = \\
&\sum_{\mu,\nu}\int_{\partial SO_l} dS\bar{M}^{a(1)}_{e,mn}(kr\bar{r}_l)\cdot\hat{\xi}_{\bar{r}_l}\times\bar{M}^{a(1)}_{e,\mu\nu}(kr\bar{r}_l)\,A_{Me\mu\nu,Me\mu'\nu'} \\
&+\sum_{\mu,\nu}\int_{\partial SO_l} dS\bar{M}^{a(1)}_{e,mn}(kr\bar{r}_l)\cdot\hat{\xi}_{\bar{r}_l}\times\bar{M}^{a(1)}_{o,\mu\nu}(kr\bar{r}_l)\,A_{Mo\mu\nu,Me\mu'\nu'} \\
&+\sum_{\mu,\nu}\int_{\partial SO_l} dS\bar{M}^{a(1)}_{e,mn}(kr\bar{r}_l)\cdot\hat{\xi}_{\bar{r}_l}\times\bar{N}^{a(1)}_{e,\mu\nu}(kr\bar{r}_l)\,A_{Ne\mu\nu,Me\mu'\nu'} \\
&+\sum_{\mu,\nu}\int_{\partial SO_l} dS\bar{M}^{a(1)}_{e,mn}(kr\bar{r}_l)\cdot\hat{\xi}_{\bar{r}_l}\times\bar{N}^{a(1)}_{o,\mu\nu}(kr\bar{r}_l)\,A_{No\mu\nu,Me\mu'\nu'}
\end{aligned} \tag{69}$$

Then, we have one integral on the LHS. This means that for fixed μ',ν', we have one coefficient b on the LHS and 4 coefficients $C's$ for each mn. Similarly, take dot product of Equation (67) with $\bar{M}^{a(1)}_{o,mn}(kr\bar{r}_l)$, $\bar{N}^{a(1)}_{e,mn}(kr\bar{r}_l)$ and $\bar{N}^{a(1)}_{o,mn}(kr\bar{r}_l)$, respectively. In total, for each mn,we have 4 integrals of b on the LHS and 16 $C's$ coefficient integrals on the RHS, giving 4 coefficients of b on the LHS and 16 coefficients $C's$ on RHS. These give us 4 equations. We let $m = 0, 1, \ldots M_{\max}, n = 1, 2, \ldots N_{\max}$, then we have $(M_{\max}+1)N_{\max} = L_{\max}$. There are $4L_{\max}$ equations in total.

Step (3): Use Equation (68) which has $\sigma' = o$. Repeat Step (2) by taking 4 dot products with $\bar{M}^{a(1)}_{e,mn}(kr\bar{r}_l)$, $\bar{M}^{a(1)}_{o,mn}(kr\bar{r}_l)$, $\bar{N}^{a(1)}_{e,mn}(kr\bar{r}_l)$ and $\bar{N}^{a(1)}_{o,mn}(kr\bar{r}_l)$, for each of them. Step (2) and step (3) will give totally $8L_{\max}$ equations.

Step (4): repeat steps (1)–(3) for $(\mu',\nu') = 1, 2, \ldots L_{\max}$. Then, totally $8L^2_{\max}$ equations are obtained for the $8L^2_{\max}$ translation addition coefficients to be solved.

The detailed calculations for all the steps are presented as below.

First, we analyze the right hand side of Equation (69). The calculations are similar to those in section 2.4, except that the outgoing vector spheroidal waves are replaced by incoming spheroidal waves. We illustrate the calculations of one term as below.

$$\begin{aligned}
C^{M,e,M,e(1)}_{mn\mu\nu} &= \int_{\partial SO}\bar{M}^{a(1)}_{e,mn}\cdot\hat{\xi}\times\bar{M}^{a(1)}_{e,\mu\nu} \\
&= \int_{\partial SO}\left(M^{a(1)}_{e,mn\eta}\hat{\eta}+M^{a(1)}_{e,mn\xi}\hat{\xi}+M^{a(1)}_{e,mn\phi}\hat{\phi}\right)\cdot\left(-M^{a(1)}_{e,\mu\nu\eta}\hat{\phi}+M^{a(1)}_{e,\mu\nu\phi}\hat{\eta}\right) \\
&= f^2\left(\xi^2-1\right)^{\frac{1}{2}}\int_0^{2\pi}d\phi\int_{-1}^{1}d\eta\left(\xi^2-\eta^2\right)^{\frac{1}{2}}\left[-M^{a(1)}_{e,\mu\nu\eta}M^{a(1)}_{e,mn\phi}+M^{a(1)}_{e,\mu\nu\phi}M^{a(1)}_{e,mn\eta}\right]
\end{aligned} \tag{70}$$

In comparison with the previous section, we note that the integrands are the products of two incoming waves. Thus, a superscript '(1)' is used to distinguish the C of this section from the C of the previous section. Because the regular incoming waves are smooth [41], we do not need to introduce the smoothing function $g(\eta)$. We next use

$$\begin{aligned}
&M^{a(1)}_{e,mn\eta} = f^{M\eta(1)}_{mn}(\eta)\sin(m\phi); M^{a(1)}_{o,mn\eta} = -f^{M\eta(1)}_{mn}(\eta)\cos(m\phi); \\
&M^{a(1)}_{e,mn\phi} = f^{M\phi(1)}_{mn}(\eta)\cos(m\phi); M^{a(1)}_{o,mn\phi} = f^{M\phi(1)}_{mn}(\eta)\sin(m\phi).
\end{aligned} \tag{71}$$

Thus,

$$\begin{aligned}
C^{M,e,M,e(1)}_{mn\mu\nu} &= f^2\left(\xi^2-1\right)^{\frac{1}{2}}\left\{\begin{array}{l}\left[\int_0^{2\pi}d\phi\sin(\mu\phi)\cos(m\phi)\int_{-1}^{1}d\eta\left(\xi^2-\eta^2\right)^{\frac{1}{2}}\left(-f^{M\eta(1)}_{\mu\nu}(\eta)f^{M\phi(1)}_{mn}(\eta)\right)\right] \\ +\left[\int_0^{2\pi}d\phi\cos(\mu\phi)\sin(m\phi)\int_{-1}^{1}d\eta\left(\xi^2-\eta^2\right)^{\frac{1}{2}}f^{M\phi(1)}_{\mu\nu}(\eta)f^{M\eta(1)}_{mn}(\eta)\right]\end{array}\right\} \\
&= 0
\end{aligned} \tag{72}$$

The 4 dot products give 4 coefficients $C_{mn\mu\nu}^{M,e,M,e(1)}$, $C_{mn\mu\nu}^{M,e,M,o(1)} C_{mn\mu\nu}^{M,e,N,e(1)}$ and $C_{mn\mu\nu}^{M,e,N,o(1)}$. Then, as described in step 2,we repeat by taking the dot product of Equation (67) with $\bar{M}_{o,mn}^{a(1)}(kr\bar{r}_l)$, $\bar{N}_{e,mn}^{a(1)}(kr\bar{r}_l)$ and $\bar{N}_{o,mn}^{a(1)}(kr\bar{r}_l)$, and obtain the 16 coefficients of $C's$.

The 16 $C_{mn\mu\nu}$ integral coefficients involve the products of the 4 vector spheroidal waves $\bar{M}_{e,mn}^{a(1)}(kr\bar{r}_l), \bar{M}_{o,mn}^{a(1)}(kr\bar{r}_l)$, $\bar{N}_{e,mn}^{a(1)}(kr\bar{r}_l)$ and $\bar{N}_{o,mn}^{a(1)}(kr\bar{r}_l)$ with the 4 vector spheroidal waves $\bar{M}_{e,\mu\nu}^{a(1)}(kr\bar{r}_l)$, $\bar{M}_{o,\mu\nu}^{a(1)}(kr\bar{r}_l)$, $\bar{N}_{e,\mu\nu}^{a(1)}(kr\bar{r}_l)$ and $\bar{N}_{o,\mu\nu}^{a(1)}(kr\bar{r}_l)$.

Because the expressions of the $C_{mn\mu\nu}$ coefficients are integrals of the products of $\bar{M}$ and $\bar{N}$ over the same surface of the l scatterer, the $\int_0^{2\pi} d\phi$ is carried out analytically. Thus we only have one dimensional integral over η for the $C_{mn\mu\nu}$ coefficients. The $C_{mn\mu\nu}^{M,e,M,e(1)}$ coefficient is given above. The one dimensional integrals of other 15 coefficients are given below.

$$C_{mn\mu\nu}^{M,e,M,o(1)} = \int_{\partial SO} \bar{M}_{e,mn}^{a(1)} \cdot \hat{\xi} \times \bar{M}_{o,\mu\nu}^{a(1)}$$
$$= \pi\delta_{\mu m} f^2 \left(\xi^2-1\right)^{\frac{1}{2}} \int_{-1}^{1} d\eta \left\{ \left(\xi^2-\eta^2\right)^{\frac{1}{2}} \left[f_{\mu\nu}^{M\eta(1)}(\eta) f_{mn}^{M\phi(1)}(\eta) + f_{\mu\nu}^{M\phi(1)}(\eta) f_{mn}^{M\eta(1)}(\eta) \right] \right\} \quad (73)$$

$$C_{mn\mu\nu}^{M,e,N,e(1)} = \int_{\partial SO} \bar{M}_{e,mn}^{a(1)} \cdot \hat{\xi} \times \bar{N}_{e,\mu\nu}^{a(1)}$$
$$= \pi\delta_{\mu m} f^2 \left(\xi^2-1\right)^{\frac{1}{2}} \int_{-1}^{1} d\eta \left\{ \left(\xi^2-\eta^2\right)^{\frac{1}{2}} \left[-f_{\mu\nu}^{N\eta(1)}(\eta) f_{mn}^{M\phi(1)}(\eta) + f_{\mu\nu}^{N\phi(1)}(\eta) f_{mn}^{M\eta(1)}(\eta) \right] \right\} \quad (74)$$

$$C_{mn\mu\nu}^{M,e,N,o(1)} = \int_{\partial SO} \bar{M}_{e,mn}^{a(1)} \cdot \hat{\xi} \times \bar{N}_{o,\mu\nu}^{a(1)} = 0 \quad (75)$$

For the notations of $C_{mn\mu\nu}^{M,e,M,e(1)}$, the first part of the super/sub scripts (Me, mn) denote the the applied dot product which in this case is $\bar{M}_{e,mn}^{a(1)}$. Th second part of the super/sub script, $(Me, \mu\nu)$ refers to the term that is inside the summation on the RHS of Equation (67).

Next, take the dot product of Equation (67) with $\bar{M}_{o,mn}^{a(1)}(kr\bar{r}_l)$ and integration over the surface of spheroidal l. Similarly, the 4 integrals on the RHS are calculated as below.

$$C_{mn\mu\nu}^{M,o,M,e(1)} = \int_{\partial SO} \bar{M}_{o,mn}^{a(1)} \cdot \hat{\xi} \times \bar{M}_{e,\mu\nu}^{a(1)}$$
$$= \pi\delta_{\mu m} f^2 \left(\xi^2-1\right)^{\frac{1}{2}} \int_{-1}^{1} d\eta \left\{ \left(\xi^2-\eta^2\right)^{\frac{1}{2}} \left[-f_{\mu\nu}^{M\eta(1)}(\eta) f_{mn}^{M\phi(1)}(\eta) - f_{\mu\nu}^{M\phi(1)}(\eta) f_{mn}^{M\eta(1)}(\eta) \right] \right\} \quad (76)$$

$$C_{mn\mu\nu}^{M,o,M,o(1)} = \int_{\partial SO} \bar{M}_{o,mn}^{a(1)} \cdot \hat{\xi} \times \bar{M}_{o,\mu\nu}^{a(1)} = 0 \quad (77)$$

$$C_{mn\mu\nu}^{M,o,N,e(1)} = \int_{\partial SO} \bar{M}_{o,mn}^{a(1)} \cdot \hat{\xi} \times \bar{N}_{e,\mu\nu}^{a(1)} = 0 \quad (78)$$

$$C_{mn\mu\nu}^{M,o,N,o(1)} = \int_{\partial SO} \bar{M}_{o,mn}^{a(1)} \cdot \hat{\xi} \times \bar{N}_{o,\mu\nu}^{a(1)}$$
$$= \pi\delta_{\mu m} f^2 \left(\xi^2-1\right)^{\frac{1}{2}} \int_{-1}^{1} d\eta \left\{ \left(\xi^2-\eta^2\right)^{\frac{1}{2}} \left[-f_{\mu\nu}^{N\eta(1)}(\eta) f_{mn}^{M\phi(1)}(\eta) + f_{\mu\nu}^{N\phi(1)}(\eta) f_{mn}^{M\eta(1)}(\eta) \right] \right\} \quad (79)$$

Next, take the dot product of Equation (67) with $\bar{N}_{e,mn}^{a(1)}(kr\bar{r}_l)$. We have

$$C_{mn\mu\nu}^{N,e,M,e(1)} = \int_{\partial SO} \bar{N}_{e,mn}^{a(1)} \cdot \hat{\xi} \times \bar{M}_{e,\mu\nu}^{a(1)}$$
$$= \pi\delta_{\mu m} f^2 \left(\xi^2-1\right)^{\frac{1}{2}} \int_{-1}^{1} d\eta \left\{ \left(\xi^2-\eta^2\right)^{\frac{1}{2}} \left[-f_{\mu\nu}^{M\eta(1)}(\eta) f_{mn}^{N\phi(1)}(\eta) + f_{\mu\nu}^{M\phi(1)}(\eta) f_{mn}^{N\eta(1)}(\eta) \right] \right\} \quad (80)$$

$$C_{mn\mu\nu}^{N,e,M,o(1)} = \int_{\partial SO} \bar{N}_{e,mn}^{a(1)} \cdot \hat{\xi} \times \bar{M}_{o,\mu\nu}^{a(1)} = 0 \quad (81)$$

$$C^{N,e,N,e(1)}_{mn\mu\nu} = \int_{\partial SO} \bar{N}^{a(1)}_{e,mn} \cdot \hat{\xi} \times \bar{N}^{a(1)}_{e,\mu\nu} = 0 \tag{82}$$

$$\begin{aligned} C^{N,e,N,o(1)}_{mn\mu\nu} &= \int_{\partial SO} \bar{N}^{a(1)}_{e,mn} \cdot \hat{\xi} \times \bar{N}^{a(1)}_{o,\mu\nu} \\ &= \pi\delta_{\mu m} f^2 \left(\xi^2-1\right)^{\frac{1}{2}} \int_{-1}^{1} d\eta \left\{ \left(\xi^2-\eta^2\right)^{\frac{1}{2}} \left[-f^{N\eta(1)}_{\mu\nu}(\eta) f^{N\phi(1)}_{mn}(\eta) - f^{N\phi(1)}_{\mu\nu}(\eta) f^{N\eta(1)}_{mn}(\eta) \right] \right\} \end{aligned} \tag{83}$$

After that, take the dot product of Equation (67) with $\bar{N}^{a(1)}_{o,mn}(kr\bar{r}_l)$.

$$C^{N,o,M,e(1)}_{mn\mu\nu} = \int_{\partial SO} \bar{N}^{a(1)}_{o,mn} \cdot \hat{\xi} \times \bar{M}^{a(1)}_{e,\mu\nu} = 0 \tag{84}$$

$$\begin{aligned} C^{N,o,M,o(1)}_{mn\mu\nu} &= \int_{\partial SO} \bar{N}^{a(1)}_{o,mn} \cdot \hat{\xi} \times \bar{M}^{a(1)}_{o,\mu\nu} \\ &= \pi\delta_{\mu m} f^2 \left(\xi^2-1\right)^{\frac{1}{2}} \int_{-1}^{1} d\eta \left\{ \left(\xi^2-\eta^2\right)^{\frac{1}{2}} \left[-f^{M\eta(1)}_{\mu\nu}(\eta) f^{N\phi(1)}_{mn}(\eta) + f^{M\phi(1)}_{\mu\nu}(\eta) f^{N\eta(1)}_{mn}(\eta) \right] \right\} \end{aligned} \tag{85}$$

$$\begin{aligned} C^{N,o,N,e(1)}_{mn\mu\nu} &= \int_{\partial SO} \bar{N}^{a(1)}_{o,mn} \cdot \hat{\xi} \times \bar{N}^{a(1)}_{e,\mu\nu} \\ &= \pi\delta_{\mu m} f^2 \left(\xi^2-1\right)^{\frac{1}{2}} \int_{-1}^{1} d\eta \left\{ \left(\xi^2-\eta^2\right)^{\frac{1}{2}} \left[f^{N\eta(1)}_{\mu\nu}(\eta) f^{N\phi(1)}_{mn}(\eta) + f^{N\phi(1)}_{\mu\nu}(\eta) f^{N\eta(1)}_{mn}(\eta) \right] \right\} \end{aligned} \tag{86}$$

$$C^{N,o,N,o(1)}_{mn\mu\nu} = \int_{\partial SO} \bar{N}^{a(1)}_{o,mn} \cdot \hat{\xi} \times \bar{N}^{a(1)}_{o,\mu\nu} = 0 \tag{87}$$

Next, we describe the 4 integrals on the left hand side giving the b coefficients.

$$\begin{aligned} b^{Me,Me(1)}_{mn\mu'\nu'} &= \int_{\partial SO_l} dS \bar{M}^{a(1)}_{e,mn}(kr\bar{r}_l) \cdot \hat{\xi}_{\bar{r}_l} \times \bar{M}^{a(3)}_{e,\mu'\nu'}(c,\xi_j,\eta_j,\phi_j) \\ &= \int_{\partial SO_l} dS \bar{M}^{a(3)}_{e,\mu'\nu'}(c,\xi_j,\eta_j,\phi_j) \cdot \left[-\hat{\xi}_{\bar{r}_l} \times \bar{M}^{a(1)}_{e,mn}(kr\bar{r}_l) \right] \\ &= \int_{\partial SO_l} dS \bar{M}^{a(3)}_{e,\mu'\nu'}(c,\xi_j,\eta_j,\phi_j) \cdot \left(M^{a(1)}_{e,mn\eta} \hat{\phi}_{\bar{r}_l} - M^{a(1)}_{e,mn\phi} \hat{\eta}_{\bar{r}_l} \right) \end{aligned} \tag{88}$$

Note that the two dimensional integration is over the spheroidal surface of spheroid l. The integrand is a product of spheroidal function centered at $\bar{r}_l$ with spheroidal functions centered at $\bar{r}_j$. Since j and l are different, we cannot do the $\int_0^{2\pi} d\phi$ integral as in the case of $C_{mn\mu\nu}$. We have two dimensional integrals of $b_{mn\mu\nu}$.

The second factor $\bar{M}^{a(3)}_{e,\mu'\ \nu'}(c,\xi_j,\eta_j,\phi_j)$ is outgoing vector spheroidal wave from spheroid j. Thus, we need to transform it from the spheroidal coordinate system centered at $\bar{r}_j$ to the spheroidal coordinate system centered at $\bar{r}_l$.

$$\begin{aligned} \bar{M}^{a(3)}_{e,\mu'\nu'}(c,\xi_j,\eta_j,\phi_j) &= M^{a(3)}_{e,\mu'\nu'\eta} \hat{\eta}_{\bar{r}_j} + M^{a(3)}_{e,\mu'\nu'\xi} \hat{\xi}_{\bar{r}_j} + M^{a(3)}_{e,\mu'\nu'\phi} \hat{\phi}_{\bar{r}_l} \\ &= M^{f_{lj},a(3)}_{e,\mu'\nu'\eta} \hat{\eta}_{\bar{r}_l} + M^{f_{lj},a(3)}_{e,\mu'\nu'\xi} \hat{\xi}_{\bar{r}_l} + M^{f_{lj},a(3)}_{e,\mu'\nu'\phi} \hat{\phi}_{\bar{r}_l} \end{aligned} \tag{89}$$

where the superscript f_{lj} indicates the coordinate transformation.

Then, $b^{Me,Me(1)}_{mn\mu'\nu'}$ is calculated as

$$b^{Me,Me(1)}_{mn\mu'\nu'} = \int_{-1}^{1} d\eta \int_0^{2\pi} d\phi f^2 \left(\xi^2-1\right)^{\frac{1}{2}} \left(\xi^2-\eta^2\right)^{\frac{1}{2}} \left(M^{f_{lj},a(3)}_{e,\mu'\nu'\phi} M^{a(1)}_{e,mn\eta} - M^{f_{lj},a(3)}_{e,\mu'\nu'\eta} M^{a(1)}_{e,mn\phi} \right) \tag{90}$$

The two dimensional integration is calculated numerically. Similarly, the other three terms of b are calculated as follows.

$$b^{Mo,Me(1)}_{mn\mu'\nu'} = \int_{-1}^{1} d\eta \int_0^{2\pi} d\phi f^2 \left(\xi^2-1\right)^{\frac{1}{2}} \left(\xi^2-\eta^2\right)^{\frac{1}{2}} \left(M^{f_{lj},a(3)}_{e,\mu'\nu'\phi} M^{a(1)}_{o,mn\eta} - M^{f_{lj},a(3)}_{e,\mu'\nu'\eta} M^{a(1)}_{o,mn\phi} \right) \tag{91}$$

$$b_{mn\mu'\nu'}^{Ne,Me(1)} = \int_{-1}^{1} d\eta \int_{0}^{2\pi} d\phi f^2 \left(\xi^2-1\right)^{\frac{1}{2}} \left(\xi^2-\eta^2\right)^{\frac{1}{2}} \left(M_{e,\mu'\nu'\phi}^{f_{lj},a(3)} N_{e,mn\eta}^{a(1)} - M_{e,\mu'\nu'\eta}^{f_{lj},a(3)} N_{e,mn\phi}^{a(1)}\right) \tag{92}$$

$$b_{mn\mu'\nu'}^{No,Me(1)} = \int_{-1}^{1} d\eta \int_{0}^{2\pi} d\phi f^2 \left(\xi^2-1\right)^{\frac{1}{2}} \left(\xi^2-\eta^2\right)^{\frac{1}{2}} \left(M_{e,\mu'\nu'\phi}^{f_{lj},a(3)} N_{o,mn\eta}^{a(1)} - M_{e,\mu'\nu'\eta}^{f_{lj},a(3)} N_{o,mn\phi}^{a(1)}\right) \tag{93}$$

For the notations of $b's$, the first super/sub script (Mo, mn) is what dot product is taken and the second super/sub script $(Me, \mu'\nu')$ refers to the left hand of the original equation before taking the dot product. Since Equation (67) has (Me) originally on the LHS, we have (Me) as the second superscript above.

The magnitude of $\bar{M}_{\sigma,mn}^{a(3)}(kr\bar{r}_j)$ is plotted on the spheroidal surface centered at $\bar{r}_l$ in Fig. 8. It is observed that $|\bar{M}_{o,01}^{r(3)}(r\bar{r}_j)| = 0$. This can be verified by substituting $m = 0$ and $n = 1$ into the expression of $\bar{M}_{o,mn}^{a(3)}$ in Appendix A.

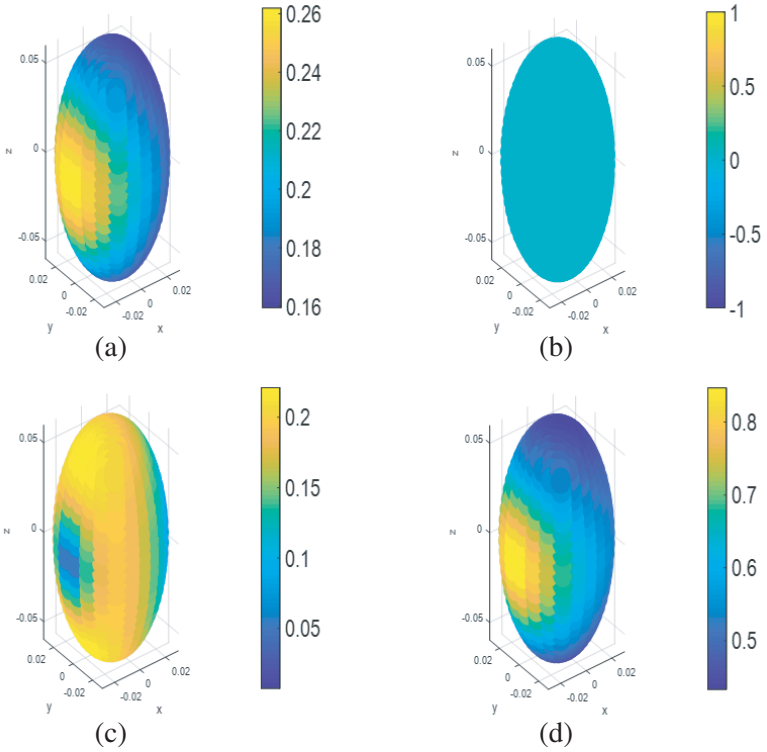

Figure 8. $|\bar{M}_{\sigma,mn}^{r(3)}(r\bar{r}_j)|$ on the spheroidal surface centered at $\bar{r}_l$, where $\bar{r}_l = [0,0,0]$, $\bar{r}_j = [-\lambda/2, 0, 0]$ for (a) $\sigma = e$, $m = 0$, $n = 1$; (b) $\sigma = o$, $m = 0$, $n = 1$; (c) $\sigma = e, m = 1, n = 2$; (d) $\sigma = o$, $m = 1$, $n = 2$.

Then, we have 4 equations

$$b_{mn\mu'\nu'}^{Me,Me} = \left[\begin{array}{l} \sum\limits_{\mu,\nu} C_{mn\mu\nu}^{M,e,M,e(1)} A_{Me\mu\nu,Me\mu'\nu'} + \sum\limits_{\mu,\nu} C_{mn\mu\nu}^{M,e,M,o(1)} A_{Mo\mu\nu,Me\mu'\nu'} \\ + \sum\limits_{\mu,\nu} C_{mn\mu\nu}^{M,e,N,e(1)} A_{Ne\mu\nu,Me\mu'\nu'} + \sum\limits_{\mu,\nu} C_{mn\mu\nu}^{M,e,N,o(1)} A_{No\mu\nu,Me\mu'\nu'} \end{array}\right] \tag{94}$$

$$b_{mn\mu'\nu'}^{Mo,Me} = \left[\begin{array}{l} \sum\limits_{\mu,\nu} C_{mn\mu\nu}^{M,o,M,e(1)} A_{Me\mu\nu,Me\mu'\nu'} + \sum\limits_{\mu,\nu} C_{mn\mu\nu}^{M,o,M,o(1)} A_{Mo\mu\nu,Me\mu'\nu'} \\ + \sum\limits_{\mu,\nu} C_{mn\mu\nu}^{M,o,N,e(1)} A_{Ne\mu\nu,Me\mu'\nu'} + \sum\limits_{\mu,\nu} C_{mn\mu\nu}^{M,o,N,o(1)} A_{No\mu\nu,Me\mu'\nu'} \end{array}\right] \tag{95}$$

$$b^{Ne,Me}_{mn\mu'\nu'} = \left[\begin{array}{l} \sum\limits_{\mu,\nu} C^{N,e,M,e(1)}_{mn\mu\nu} A_{Me\mu\nu,Me\mu'\nu'} + \sum\limits_{\mu,\nu} C^{N,e,M,o(1)}_{mn\mu\nu} A_{Mo\mu\nu,Me\mu'\nu'} \\ + \sum\limits_{\mu,\nu} C^{N,e,N,e(1)}_{mn\mu\nu} A_{Ne\mu\nu,Me\mu'\nu'} + \sum\limits_{\mu,\nu} C^{N,e,N,o(1)}_{mn\mu\nu} A_{No\mu\nu,Me\mu'\nu'} \end{array} \right] \tag{96}$$

$$b^{No,Me}_{mn\mu'\nu'} = \left[\begin{array}{l} \sum\limits_{\mu,\nu} C^{N,o,M,e(1)}_{mn\mu\nu} A_{Me\mu\nu,Me\mu'\nu'} + \sum\limits_{\mu,\nu} C^{N,o,M,o(1)}_{mn\mu\nu} A_{Mo\mu\nu,Me\mu'\nu'} \\ + \sum\limits_{\mu,\nu} C^{N,o,N,e(1)}_{mn\mu\nu} A_{Ne\mu\nu,Me\mu'\nu'} + \sum\limits_{\mu,\nu} C^{N,o,N,o(1)}_{mn\mu\nu} A_{No\mu\nu,Me\mu'\nu'} \end{array} \right] \tag{97}$$

In the above 4 equations, we let (μ', ν') and (m, n) be $1, 2, ...L_{\max}$. Thus we have $4L^2_{\max}$ equations.

Next, we use Equation (68), $\sigma' = o$ and have $(Mo, \mu'\nu')$ on the LHS. We take the dot products with $\bar{M}^{a(1)}_{e,mn}(kr\bar{r}_l)$, $\bar{M}^{a(1)}_{o,mn}(kr\bar{r}_l)$, $\bar{N}^{a(1)}_{e,mn}(kr\bar{r}_l)$ and $\bar{N}^{a(1)}_{o,mn}(kr\bar{r}_l)$. We get $4L^2_{\max}$ equations.

Note that the LHS is changed from the Equation (69) of step (2) because we have $\sigma' = o$ on the LHS. On the RHS, the translation coefficients $A's$ depend on σ' and are changed from the Equation (69) of step (2). However, the 16 $C_{mn\mu\nu}$ integral coefficients remain the same between step (2) and step (3) because they only depend on the products of $\bar{M}^{a(1)}_{e,mn}(kr\bar{r}_l)$, $\bar{M}^{a(1)}_{o,mn}(kr\bar{r}_l)$, $\bar{N}^{a(1)}_{e,mn}(kr\bar{r}_l)$ and $\bar{N}^{a(1)}_{o,mn}(kr\bar{r}_l)$ with $\bar{M}^{a(1)}_{e,\mu\nu}(kr\bar{r}_l)$, $\bar{M}^{a(1)}_{o,\mu\nu}(kr\bar{r}_l)$, $\bar{N}^{a(1)}_{e,\mu\nu}(kr\bar{r}_l)$ and $\bar{N}^{a(1)}_{o,\mu\nu}(kr\bar{r}_l)$.

Following the same procedures as those for Equation (67), we obtain the 4 equations

$$b^{Me,Mo}_{mn\mu'\nu'} = \left[\begin{array}{l} \sum\limits_{\mu,\nu} C^{M,e,M,e(1)}_{mn\mu\nu} A_{Me\mu\nu,Mo\mu'\nu'} + \sum\limits_{\mu,\nu} C^{M,e,M,o(1)}_{mn\mu\nu} A_{Mo\mu\nu,Mo\mu'\nu'} \\ + \sum\limits_{\mu,\nu} C^{M,e,N,e(1)}_{mn\mu\nu} A_{Ne\mu\nu,Mo\mu'\nu'} + \sum\limits_{\mu,\nu} C^{M,e,N,o(1)}_{mn\mu\nu} A_{No\mu\nu,Mo\mu'\nu'} \end{array} \right] \tag{98}$$

$$b^{Mo,Mo}_{mn\mu'\nu'} = \left[\begin{array}{l} \sum\limits_{\mu,\nu} C^{M,o,M,e(1)}_{mn\mu\nu} A_{Me\mu\nu,Mo\mu'\nu'} + \sum\limits_{\mu,\nu} C^{M,o,M,o(1)}_{mn\mu\nu} A_{Mo\mu\nu,Mo\mu'\nu'} \\ + \sum\limits_{\mu,\nu} C^{M,o,N,e(1)}_{mn\mu\nu} A_{Ne\mu\nu,Mo\mu'\nu'} + \sum\limits_{\mu,\nu} C^{M,o,N,o(1)}_{mn\mu\nu} A_{No\mu\nu,Mo\mu'\nu'} \end{array} \right] \tag{99}$$

$$b^{Ne,Mo}_{mn\mu'\nu'} = \left[\begin{array}{l} \sum\limits_{\mu,\nu} C^{N,e,M,e(1)}_{mn\mu\nu} A_{Me\mu\nu,Mo\mu'\nu'} + \sum\limits_{\mu,\nu} C^{N,e,M,o(1)}_{mn\mu\nu} A_{Mo\mu\nu,Mo\mu'\nu'} \\ + \sum\limits_{\mu,\nu} C^{N,e,N,e(1)}_{mn\mu\nu} A_{Ne\mu\nu,Mo\mu'\nu'} + \sum\limits_{\mu,\nu} C^{N,e,N,o(1)}_{mn\mu\nu} A_{No\mu\nu,Mo\mu'\nu'} \end{array} \right] \tag{100}$$

$$b^{No,Mo}_{mn\mu'\nu'} = \left[\begin{array}{l} \sum\limits_{\mu,\nu} C^{N,o,M,e(1)}_{mn\mu\nu} A_{Me\mu\nu,Mo\mu'\nu'} + \sum\limits_{\mu,\nu} C^{N,o,M,o(1)}_{mn\mu\nu} A_{Mo\mu\nu,Mo\mu'\nu'} \\ + \sum\limits_{\mu,\nu} C^{N,o,N,e(1)}_{mn\mu\nu} A_{Ne\mu\nu,Mo\mu'\nu'} + \sum\limits_{\mu,\nu} C^{N,o,N,o(1)}_{mn\mu\nu} A_{No\mu\nu,Mo\mu'\nu'} \end{array} \right] \tag{101}$$

For the notations of $b's$, the first super/sub script (Mo, mn) is what dot product is taken, and the second super/sub script $(Me, \mu'\nu')$ refers to the left hand of the original equation before taking the dot product. Since Equation (68) has (Mo) originally on the LHS, we have (Mo) as the second superscript above. Note that we do not have (Ne) nor (No) as second superscript on the LHS because we only use the equation of $\bar{M}^{a(3)}_{\sigma',\mu'\nu'}(c, \xi_j, \eta_j, \phi_j)$ and we do not use the equation of $\bar{N}^{a(3)}_{\sigma',\mu'\nu'}(c, \xi_j, \eta_j, \phi_j)$ in (66).

We have described the $8L^2_{\max}$ equations, the $8L^2_{\max}$ number of $A's$ to be determined, and the 16 expressions for the integrals $C's$. Next we introduce compact notaions.

For the four Equations (94), (95), (98), and (99), we use combined index notations that $(\sigma, \mu\nu) \rightarrow \alpha = 1, 2, \ldots, 2L_{\max}$. The factor of 2 is that we now include $\sigma = e, o$ in the combined index.

We take the Equations (94) and (95) of step (2) from Equation (67) ($\sigma' = e$) and the Equations (98) and (99) of step (3) from Equation (68) ($\sigma' = o$). In these cases, we take the dot product with $\bar{M}^{a(1)}_{e,mn}(kr\bar{r}_l)$ and $\bar{M}^{a(1)}_{o,mn}(kr\bar{r}_l)$,

$$b^{M\beta,M\alpha'} = \sum_{\alpha} C^{M\beta,M\alpha} A_{M\alpha,M\alpha'} + \sum_{\alpha} C^{M\beta,N\alpha} A_{N\alpha,M\alpha'} \tag{102}$$

where $\beta = (\sigma, m, n)\,; \alpha = (\sigma, \mu, \nu)\,; \alpha' = (\sigma', \mu', \nu')$.

In matrix notations,

$$\overset{=MM}{b} = \overset{=MM}{C}\overset{=MM}{A} + \overset{=MN}{C}\overset{=NM}{A} \tag{103}$$

where all matrices are of sizes $(2L_{\max}) \times (2L_{\max})$.

Then, we take the Equations (96) and (97) of step (2) from Equation (67) ($\sigma' = e$) and the Equations (100) and (101) of step (3) from Equation (68) ($\sigma' = o$). Then,

$$b^{N\beta,M\alpha'} = \sum_{\alpha} C^{N\beta,M\alpha} A_{M\alpha,M\alpha'} + \sum_{\alpha} C^{N\beta,N\alpha} A_{N\alpha,M\alpha'} \tag{104}$$

where $\beta = (\sigma, m, n)\,; \alpha = (\sigma, \mu, \nu)\,; \alpha' = (\sigma', \mu', \nu')$.

In matrix form,

$$\overset{=NM}{b} = \overset{=NM}{C}\overset{=NM}{A} + \overset{=NN}{C}\overset{=NM}{A} \tag{105}$$

where all matrices are of sizes $(2L_{\max}) \times (2L_{\max})$.

Combining the two matrices form equations, we have

$$\begin{bmatrix} \overset{=MM}{b} \\ \overset{=NM}{b} \end{bmatrix} = \begin{bmatrix} \overset{=MM}{C} & \overset{=MN}{C} \\ \overset{=NM}{C} & \overset{=NN}{C} \end{bmatrix} \begin{bmatrix} \overset{=MM}{A} \\ \overset{=NM}{A} \end{bmatrix} \tag{106}$$

Then, the translational addition coefficients are calculated by taking the inverse of the C matrix,

$$\begin{bmatrix} \overset{=MM}{A} \\ \overset{=NM}{A} \end{bmatrix} = \begin{bmatrix} \overset{=MM}{C} & \overset{=MN}{C} \\ \overset{=NM}{C} & \overset{=NN}{C} \end{bmatrix}^{-1} \begin{bmatrix} \overset{=MM}{b} \\ \overset{=NM}{b} \end{bmatrix} \tag{107}$$

5. RESULTS AND DISCUSSIONS ON NUMERICAL TRANSLATION ADDITION FOR VECTOR SPHEROIDAL WAVES

For vector spheroidal waves, there is no analytical translation addition theorem available for general cases. However, the $\bar{\bar{C}}$ matrix needed in the numerical translation addition method as in Equation (58)

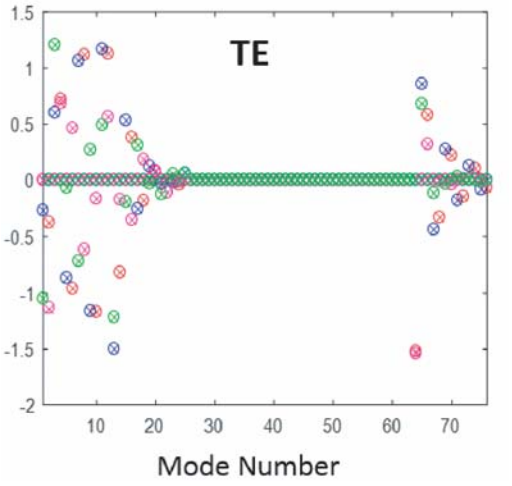

Figure 9. Vector spheroidal wave expansion coefficients for incident plane waves using numerical method (maker of cross) and analytical method (maker of circle) for TE polarization.

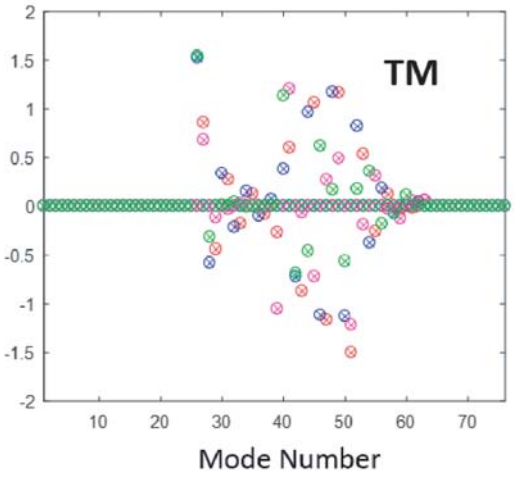

Figure 10. Vector spheroidal wave expansion coefficients for incident plane waves using numerical method (maker of cross) and analytical method (maker of circle) for TM polarization.

can be verified. To verify $\bar{\bar{C}}$, we replace $\bar{M}_{mn}(kr\bar{r}_2)$ by incident plane wave $\bar{E}^{inc}$ in the numerical translation addition method. With the same $\bar{\bar{C}}$, when $\bar{b}$ is integrated using $\bar{E}^{inc}$, the resulting $\bar{A}$ and $\bar{B}$ are the expansion coefficients for incident plane waves. For incident plane waves, the analytical solutions of the expansion coefficients are available as listed in Section 2. Fig. 9 and Fig. 10 show a comparison between the expansion coefficients from the numerical method and the analytical solutions for TE and TM polarizations, respectively. The incident plane waves are of $\phi_i = 0$ and $\theta_i = 10^\circ$ and 40°. For $\theta_i = 10^\circ$, the real part of the expansion coefficient is in red while the imaginary part is in blue. For $\theta_i = 40^\circ$, the real part of the expansion coefficient is in magenta while the imaginary part is in green. The circle marker indicates the results of the analytical method while the cross marker indicates the results of the numerical method. The results from analytical and the numerical method matches well. This means that the $\bar{\bar{C}}$ and the way of calculating $\bar{b}$ for the translation addition method is correct.

6. CONCLUSIONS

This paper developed the numerical methods of calculations of T-matrix and vector translation addition coefficients using vector spherical and spheroidal waves, for multiple scattering of waves by complex objects. The numerical T-matrix extraction technique is applicable to complex objects such as branches with leaves. The T-matrix calculation technique for the vector spheroidal waves is much complicated compared to the vector spherical waves because the vector spheroidal waves have no orthogonality property in the $\hat{\eta}$ direction. The smoothing function is also introduced for the outgoing spheroidal waves to remove their singularities. The accuracy of the extracted T-matrix with vector spheroidal wave expansions is verified by comparing the scattered fields computed from the T-matrix to those from the commercial software HFSS, for a branch with leaves. The numerical method is more robust than the analytical method. The translation coefficients transform the outgoing spheroidal waves from one object to the incoming spheroidal waves to the other object. The derivations of the numerical transformation coefficients for vector spheroidal waves are presented in this paper. The accuracy of the numerical method of calculating the transformation coefficients for vector spheroidal waves is verified. The generalized numerical T-matrix extraction and vector wave transformations are the two key steps in the hybrid method of calculating multiple scatterings. The numerical T-matrix extraction and wave transformation techniques for vector spheroidal waves will be used in the hybrid method to calculate the multiple scattering of complex objects.

ACKNOWLEDGMENT

The research described in this paper was carried out at the University of Michigan, Ann Arbor, MI 48109, USA, and was supported in part by the Jet Propulsion Laboratory, California Institute of Technology, under a contract with the National Aeronautics and Space Administration.

APPENDIX A.

A.1. Vector Spheroidal Functions

In this appendix, the calculations of vector spheroidal functions [42] are reviewed, which are important to obtain the results in this paper.

The prolate spheroidal scalar wave function is

$$\psi_{mn} = S_{mn}(c,\eta)R_{mn}(c,\xi) \begin{matrix}\sin\\ \cos\end{matrix} (m\phi) \tag{A1}$$

where $c = \frac{1}{2}kd$. $sin(m\phi)$ are the odd modes while $cos(m\phi)$ are the even modes, which are used instead of $exp(im\phi)$ to follow the formulations in [32]. $S_{mn}(c,\eta)$ is the spheroidal angular function, and $R_{mn}(c,\xi)$ is the spheroidal radial function.

The spheroidal angular function $S_{mn}(c,\eta)$ satisfies the following equation,

$$\frac{d}{d\eta}\left[\left(1-\eta^2\right)\frac{d}{d\eta}S_{mn}(c,\eta)\right] + \left[\lambda_{mn} - c^2\eta^2 - \frac{m^2}{1-\eta^2}\right]S_{mn}(c,\eta) = 0 \tag{A2}$$

where λ_{mn} is the characteristic value. There are two linearly independent solutions to this equation. One is spheroidal angular function of the first kind

$$S_{mn}^{(1)}(c,\eta) = \sum_{r=0,1}^{\infty} {}' d_r^{mn}(c) P_{m+r}^m(\eta) \tag{A3}$$

where $P_{m+r}^m(\eta)$ is the associated Legendre function of the first kind. The prime on the summation means that the summation is over even r when $(n-m)$ is even and over odd r when $(n-m)$ is odd. In this section, only prolate spheroidal function is used and thus only $S_{mn}(c,\eta)$ is needed. For simplification, the superscript '(1)' is omitted later in this section.

The coefficient d_r^{mn} can be calculated using the following formula,

$$A_r^m(c) d_{r+2}^{mn}(c) + \left[B_r^m(c) - \lambda_{mn}(c)\right] d_r^{mn}(c) + C_r^m(c) d_{r-2}^{mn}(c) = 0 \tag{A4}$$

The detailed steps of calculations can be found in [41, 42].

The spheroidal radial function $R_{mn}(c,\xi)$ satisfies the following equation

$$\frac{d}{d\xi}\left[\left(\xi^2-1\right)\frac{d}{d\xi}R_{mn}(c,\xi)\right] - \left[\lambda_{mn} - c^2\xi^2 + \frac{m^2}{\xi^2-1}\right] R_{mn}(c,\xi) = 0 \tag{A5}$$

The solution is as follows

$$R_{mn}^{(i)}(c,\xi) = \left[\sum_{r=0,1}^{\infty} {}' i^{r+m-n} d_r^{mn}(c) \frac{(2m+r)!}{r!} Z_{m+r}^{(i)}(c\xi)\right] \frac{\left(\dfrac{\xi^2-1}{\xi^2}\right)^{m/2}}{\displaystyle\sum_{r=0,1}^{\infty} {}' d_r^{mn}(c) \frac{(2m+r)!}{r!}} \tag{A6}$$

where $i = 1, 2, 3, 4$ with $z_n^{(1)}(x) = j_n(x), z_n^{(2)}(x) = n_n(x), z_n^{(3)}(x) = h_n^{(1)}(x), z_n^{(4)}(x) = h_n^{(2)}(x)$.

Thus,

$$\begin{aligned} R_{mn}^{(3)}(c,\xi) &= R_{mn}^{(1)}(c,\xi) + iR_{mn}^{(2)}(c,\xi) \\ R_{mn}^{(4)}(c,\xi) &= R_{mn}^{(1)}(c,\xi) - iR_{mn}^{(2)}(c,\xi) \end{aligned} \tag{A7}$$

The vector spheroidal wave functions are calculated from the scalar wave functions as below

$$\bar{M}_{(e,o)mn}^{a(i)}(c;\eta,\xi,\phi) = \nabla \times \left[\psi_{(e,o)mn}^{(i)} \hat{a}\right] \tag{A8}$$

$$\bar{N}_{(e,o)mn}^{a(i)}(c;\eta,\xi,\phi) = \frac{1}{k}\nabla \times \nabla \times \left[\psi_{(e,o)mn}^{(i)} \hat{a}\right] \tag{A9}$$

where $\hat{a}$ is $\hat{x}$, $\hat{y}$, $\hat{z}$, or $\hat{r}$.

In this paper, we use $\hat{r}$. The expressions for the vector prolate spheroidal wave functions are as follows [42]

$$\bar{M}_{(e,o)mn}^{r(i)} = M_{(e,o)m,n,\eta}^{r(i)} \hat{\eta} + M_{(e,o)m,n,\xi}^{r(i)} \hat{\xi} + M_{(e,o)m,n,\phi}^{r(i)} \hat{\phi} \tag{A10}$$

with

$$M_{(e,o)m,n,\eta}^{r(i)} = \frac{m\xi}{(\xi^2-\eta^2)^{\frac{1}{2}}(1-\eta^2)^{\frac{1}{2}}} S_{mn} R_{mn}^{(i)} \begin{bmatrix} \sin \\ -\cos \end{bmatrix} (m\phi) \tag{A11}$$

$$M_{(e,o)m,n,\xi}^{r(i)} = \frac{-m\eta}{(\xi^2-\eta^2)^{\frac{1}{2}}(\xi^2-1)^{\frac{1}{2}}} S_{mn} R_{mn}^{(i)} \begin{bmatrix} \sin \\ -\cos \end{bmatrix} (m\phi) \tag{A12}$$

$$M_{(e,o)m,n,\phi}^{r(i)} = \frac{\left(\xi^2-1\right)^{\frac{1}{2}}\left(1-\eta^2\right)^{\frac{1}{2}}}{\xi^2-\eta^2} \left[\xi \frac{dS_{mn}}{d\eta} R_{mn}^{(i)} - \eta S_{mn} \frac{dR_{mn}^{(i)}}{d\xi}\right] \begin{bmatrix} \cos \\ \sin \end{bmatrix} (m\phi). \tag{A13}$$

$$\bar{N}_{(e,o)mn}^{r(i)} = N_{(e,o)m,n,\eta}^{r(i)} \hat{\eta} + N_{(e,o)m,n,\xi}^{r(i)} \hat{\xi} + N_{(e,o)m,n,\phi}^{r(i)} \hat{\phi} \tag{A14}$$

with

$$N^{r(i)}_{(e,o)m,n,\eta} = \frac{2\left(1-\eta^2\right)^{\frac{1}{2}}}{kd(\xi^2-\eta^2)^{\frac{1}{2}}} \left[\begin{array}{l} \dfrac{dS_{mn}}{d\eta}\dfrac{\partial}{\partial\xi}\left(\dfrac{\xi\left(\xi^2-1\right)}{\xi^2-\eta^2}R^{(i)}_{mn}\right) \\ -\eta S_{mn}\dfrac{\partial}{\partial\xi}\left(\dfrac{\xi^2-1}{\xi^2-\eta^2}\dfrac{dR^{(i)}_{mn}}{d\xi}\right)+\dfrac{m^2\eta}{\left(1-\eta^2\right)\left(\xi^2-1\right)}S_{mn}R^{(i)}_{mn} \end{array} \right] \left[\begin{array}{l} \cos \\ \sin \end{array} (m\phi)\right] \tag{A15}$$

$$N^{r(i)}_{(e,o)m,n,\xi} = -\frac{2\left(\xi^2-1\right)^{\frac{1}{2}}}{kd(\xi^2-\eta^2)^{\frac{1}{2}}} \left[\begin{array}{l} -\dfrac{\partial}{\partial\eta}\left(\dfrac{\eta\left(1-\eta^2\right)}{\xi^2-\eta^2}S_{mn}\right)\dfrac{dR^{(i)}_{mn}}{d\xi} \\ +\xi\dfrac{\partial}{\partial\eta}\left(\dfrac{1-\eta^2}{\xi^2-\eta^2}\dfrac{dS_{mn}}{d\eta}\right)R^{(i)}_{mn}-\dfrac{m^2\xi}{\left(1-\eta^2\right)\left(\xi^2-1\right)}S_{mn}R^{(i)}_{mn} \end{array} \right] \left[\begin{array}{l} \cos \\ \sin \end{array} (m\phi)\right] \tag{A16}$$

$$N^{r(i)}_{(e,o)m,n,\phi} = \frac{2m\left(1-\eta^2\right)^{\frac{1}{2}}\left(\xi^2-1\right)^{\frac{1}{2}}}{kd\left(\xi^2-\eta^2\right)}\left[\frac{-1}{\xi^2-1}\frac{d}{d\eta}\left(\eta S_{mn}\right)R^{(i)}_{mn}-\frac{1}{1-\eta^2}S_{mn}\frac{d}{d\xi}\left(\xi R^{(i)}_{mn}\right)\right]\left[\begin{array}{l} \sin \\ -\cos \end{array} (m\phi)\right] \tag{A17}$$

where the upper function of $(m\phi)$ is for even function while the lower one is for odd function. S_{mn} is the function of η, and $R^{(1)}_{mn}$ is the function of ξ which are not written out explicitly for simplicity.

A.2. Expressions for f Functions

The f functions used in this paper are summarized below.

For outgoing spheroidal waves,

$$f^{M\eta}_{mn}(\eta) = \frac{m\xi}{(\xi^2-\eta^2)^{\frac{1}{2}}(1-\eta^2)^{\frac{1}{2}}}S_{mn}R^{(3)}_{mn} \tag{A18}$$

$$f^{M\phi}_{mn}(\eta) = \frac{\left(\xi^2-1\right)^{\frac{1}{2}}\left(1-\eta^2\right)^{\frac{1}{2}}}{\xi^2-\eta^2}\left[\xi\frac{dS_{mn}}{d\eta}R^{(3)}_{mn}-\eta S_{mn}\frac{dR^{(3)}_{mn}}{d\xi}\right] \tag{A19}$$

$$f^{N\eta}_{mn}(\eta) = \frac{2\left(1-\eta^2\right)^{\frac{1}{2}}}{kd(\xi^2-\eta^2)^{\frac{1}{2}}} \left[\begin{array}{l} \dfrac{dS_{mn}}{d\eta}\left(\left(\dfrac{\xi\left(\xi^2-1\right)}{\xi^2-\eta^2}\right)\dfrac{dR^{(3)}_{mn}}{d\xi}+\left(\dfrac{\left(\xi^4+\xi^2\right)-\left(3\xi^2-1\right)\eta^2}{\left(\xi^2-\eta^2\right)^2}\right)R^{(3)}_{mn}\right) \\ -\eta S_{mn}\left(\left(\dfrac{\xi^2-1}{\xi^2-\eta^2}\right)\dfrac{d^2R^{(3)}_{mn}}{d\xi^2}+\left(\dfrac{2\xi\left(1-\eta^2\right)}{\left(\xi^2-\eta^2\right)^2}\right)\dfrac{dR^{(3)}_{mn}}{d\xi}\right) \\ +\dfrac{m^2\eta}{\left(1-\eta^2\right)\left(\xi^2-1\right)}S_{mn}R^{(3)}_{mn} \end{array} \right] \tag{A20}$$

$$f^{N\phi}_{mn}(\eta) = \frac{2m\left(1-\eta^2\right)^{\frac{1}{2}}\left(\xi^2-1\right)^{\frac{1}{2}}}{kd\left(\xi^2-\eta^2\right)} \left[\begin{array}{l} \dfrac{-1}{\xi^2-1}\left(S_{mn}+\eta\dfrac{dS_{mn}}{d\eta}\right)R^{(3)}_{mn} \\ -\dfrac{1}{1-\eta^2}S_{mn}\left(R^{(3)}_{mn}+\xi\dfrac{dR^{(3)}_{mn}}{d\xi}\right) \end{array} \right] \tag{A21}$$

For incoming spheroidal waves,

$$f^{M\eta(1)}_{mn}(\eta) = \frac{m\xi}{(\xi^2-\eta^2)^{\frac{1}{2}}(1-\eta^2)^{\frac{1}{2}}}S_{mn}R^{(1)}_{mn} \tag{A22}$$

$$f^{M\phi(1)}_{mn}(\eta) = \frac{\left(\xi^2-1\right)^{\frac{1}{2}}\left(1-\eta^2\right)^{\frac{1}{2}}}{\xi^2-\eta^2}\left[\xi\frac{dS_{mn}}{d\eta}R^{(1)}_{mn}-\eta S_{mn}\frac{dR^{(1)}_{mn}}{d\xi}\right] \tag{A23}$$

$$f_{mn}^{N\eta(1)}(\eta) = \frac{2\left(1-\eta^2\right)^{\frac{1}{2}}}{kd(\xi^2-\eta^2)^{\frac{1}{2}}} \left[\begin{array}{l} \frac{dS_{mn}}{d\eta}\left(\left(\frac{\xi\left(\xi^2-1\right)}{\xi^2-\eta^2}\right)\frac{dR_{mn}^{(1)}}{d\xi}+\left(\frac{\left(\xi^4+\xi^2\right)-\left(3\xi^2-1\right)\eta^2}{\left(\xi^2-\eta^2\right)^2}\right)R_{mn}^{(1)}\right) \\ -\eta S_{mn}\left(\left(\frac{\xi^2-1}{\xi^2-\eta^2}\right)\frac{d^2R_{mn}^{(1)}}{d\xi^2}+\left(\frac{2\xi\left(1-\eta^2\right)}{\left(\xi^2-\eta^2\right)^2}\right)\frac{dR_{mn}^{(1)}}{d\xi}\right) \\ +\frac{m^2\eta}{\left(1-\eta^2\right)\left(\xi^2-1\right)}S_{mn}R_{mn}^{(1)} \end{array} \right] \tag{A24}$$

$$f_{mn}^{N\phi(1)}(\eta) = \frac{2m\left(1-\eta^2\right)^{\frac{1}{2}}\left(\xi^2-1\right)^{\frac{1}{2}}}{kd\left(\xi^2-\eta^2\right)} \left[\begin{array}{l} \frac{-1}{\xi^2-1}\left(S_{mn}+\eta\frac{dS_{mn}}{d\eta}\right)R_{mn}^{(1)} \\ -\frac{1}{1-\eta^2}S_{mn}\left(R_{mn}^{(1)}+\xi\frac{dR_{mn}^{(1)}}{d\xi}\right) \end{array} \right] \tag{A25}$$

REFERENCES

1. Tsang, L., J. A. Kong, and R. T. Shin, *Theory of Microwave Remote Sensing*, Wiley, New York, 1985.
2. Chandrasekhar, S., *Radiative Transfer*, Courier Corporation, 2013.
3. Ishimaru, A., *Electromagnetic Wave Propagation, Radiation, and Scattering: From Fundamentals to Applications*, John Wiley and Sons, 2017.
4. Mishchenko, M. I., L. D. Travis, and A. A. Lacis, *Multiple Scattering of Light by Particles: Radiative Transfer and Coherent Backscattering*, Cambridge University Press, 2006.
5. Ulaby, F. T., K. Sarabandi, K. Y. Mcdonald, M. Whitt, and M. C. Dobson, "Michigan microwave canopy scattering model," *International Journal of Remote Sensing*, Vol. 11, No. 7, 1223–1253, 1990.
6. Liao, T. H., S. B. Kim, S. Tan, L. Tsang, C. Su, and T. J. Jackson, "Multiple scattering effects with cyclical correction in active remote sensing of vegetated surface using vector radiative transfer theory," *IEEE Journal of Selected Topics in Applied Earth Observations and Remote Sensing*, Vol. 9, No. 4, 1414–1429, 2016.
7. Lang, R. H. and J. S. Sighu, "Electromagnetic backscattering from a layer of vegetation: A discrete approach," *IEEE Transactions on Geoscience and Remote Sensing*, Vol. 1, No. 1, 62–71, 1983.
8. Chauhan, N. S., R. H. Lang, and K. J. Ranson, "Radar modeling of a boreal forest," *IEEE Transactions on Geoscience and Remote Sensing*, Vol. 29, No. 4, 627–638, 1991.
9. Kim, S. B., J. J. Van Zyl, and et al., "Surface soil moisture retrieval using the L-band synthetic aperture radar onboard the soil moisture active-passive satellite and evaluation at core validation sites," *IEEE Transactions on Geoscience and Remote Sensing*, Vol. 55, No. 4, 1897–1914, 2017.
10. Huang, H., T.-H. Liao, L. Tsang, E. G. Njoku, A. Colliander, T. J. Jackson, M. S. Burgin, and S. Yueh, "Modelling and validation of combined active and passive microwave remote sensing of agricultural vegetation at L-band," *Progress In Electromagnetics Research B*, Vol. 78, 94–124, 2017.
11. Frisch, U., *Wave Propagation in Random Media*, Institue d'Astrophysique Centre National de la Recherche, Paris, Academic Press Inc., New York, 1968.
12. Tsang, L. and J. A. Kong, *Scattering of Electromagnetic Waves: Advanced Topics*, John Wiley and Sons, 2004.
13. Tsang, L. and A. Ishimaru, "Theory of backscattering enhancement of random discrete isotropic scatterers based on the summation of all ladder and cyclical terms," *JOSA A*, Vol. 2, No. 8, 1331–1338, 1985.
14. Tsang, L., J. A. Kong, and C. O. Ao, *Scattering of Electromagnetic Waves: Numerical Simulations*, John Wiley and Sons, 2004.

15. Tsang, L., C. E. Mandt, and K. H. Ding, "Monte Carlo simulations of the extinction rate of dense media with randomly distributed dielectric spheres based on solution of Maxwell's equations," *Optics letters*, Vol. 17, 314–316, 1992.
16. Xu, X., D. Liang, et al., "Active remote sensing of snow using NMM3D/DMRT and comparison with CLPX II airborne data," *IEEE Journal of Selected Topics in Applied Earth Observations and Remote Sensing*, Vol. 3, 689–697, 2010.
17. Tsang, L., H. Chen, C. C. Huang, and V. Jandhyala, "Modeling of multiple scattering among vias in planar waveguides using Foldy-Lax equations," *Microwave and Optical Technology Letters*, Vol. 31, 201–208, 2001.
18. Huang, H., L. Tsang, E. G. Njoku, A. Colliander, T.-H. Liao, and K. H. Ding, "Propagation and scattering by a layer of randomly distributed dielectric cylinders using Monte Carlo simulations of 3D Maxwell equations with applications in microwave interactions with vegetation," *IEEE Access*, Vol. 5, 11985–12003, 2017.
19. Huang, H., L. Tsang, A. Colliander, and S. Yueh, "Propagation of waves in randomly distributed cylinders using three-dimensional vector cylindrical wave expansions in Foldy-Lax equations," *IEEE Journal on Multiscale and Multiphysics Computational Techniques*, Vol. 4, 214–226, 2019.
20. Ulaby, F. T., D. G. Long, et al., *Microwave Radar and Radiometric Remote Sensing*, The University of Michigan, 2014.
21. Gu, W. and L. Tsang, "Vegetation effects for remote sensing of soil moisture using NMM3D full-wave simulation," *IEEE Antennas and Propagation Sympsium*, Montreal, 2020.
22. Waterman, P. C. and R. Truell, "Multiple scattering of waves," *Journal of Mathematical Physics*, Vol. 2, 512–537, 1961.
23. Peterson, B. and S. Ström, "T-matrix for electromagnetic scattering from an arbitrary number of scatterers and representations of E(3)," *Physical Review D*, Vol. 8, 3661, 1973.
24. Tse, K. K., L. Tsang, C. H. Chan, K. H. Ding, and K. W. Leung, "Multiple scattering of waves by dense random distributions of sticky particles for applications in microwave scattering by terrestrial snow," *Radio Science*, Vol. 42, 1–14, 2007.
25. Tsang, L., K. H. Ding, G. Zhang, C. C. Hsu, and J. A. Kong, "Backscattering enhancement and clustering effects of randomly distributed dielectric cylinders overlying a dielectric half space based on Monte-Carlo simulations," *IEEE Transactions on Antennas and Propagation*, Vol. 43, No. 5, 488–499, 1995.
26. Valagiannopoulos, C. A. and N. L. Tsitsas, "Linearization of the T-matrix solution for quasi-homogeneous scatterers," *JOSA A*, Vol. 26, No. 4, 870–881, 2009.
27. Maystre, D., "Electromagnetic scattering by a set of objects: An integral method based on scattering operator," *Progress In Electromagnetics Research*, Vol. 57, 55–84, 2006.
28. Valagiannopoulos, C. A., "A novel methodology for estimating the permittivity of a specimen rod at low radio frequencies," *Journal of Electromagnetic Waves and Applications*, Vol. 24, No. 5–6, 631–640, 2010.
29. Hajihashemi, M. R. and M. El-Shenawee, "Inverse scattering of three-dimensional PEC objects using the level-set method," *Progress In Electromagnetics Research*, Vol. 116, 23–47, 2011.
30. Wei, Z. and X. Chen, "Physics-inspired convolutional neural network for solving full-wave inverse scattering problems," *IEEE Transactions on Antennas and Propagation*, Vol. 67, No. 9, 6138–6148, 2019.
31. Tsang, L., J. A. Kong, and K.-H. Ding, *Scattering of Electromagnetic Waves: Theories and Applications*, John Wiley and Sons, 2004.
32. Flammer, C., *Spheroidal Wave Functions*, Courier Corporation, 2014.
33. Huang, H., "Vegetation/forest effects in microwave remote sensing of soil moisture," *Ph.D. Thesis*, 2019.
34. Sinha, B. P. and R. H. MacPhie, "Electromagnetic scattering by prolate spheroids for plane waves with arbitrary polarization and angle of incidence," *Radio Science*, Vol. 12, No. 2, 171–184, 1977.

35. Cooray, M. F. R. and I. R. Ciric, "Scattering by systems of spheroids in arbitrary configurations," *Computer Physics Communications*, Vol. 68, Nos. 1–3, 279–305, 1991.
36. Nag, S. and B. P. Sinha, "Electromagnetic plane wave scattering by a system of two uniformly lossy dielectric prolate spheroids in arbitrary orientation," *IEEE Transactions on Antennas and Propagation*, Vol. 43, No. 3, 322–327, 1995.
37. Huang, H., L. Tsang, A. Colliander, R. Shah, X. Xu, E. G. Njoku, and S. Yueh, "Numerical 3D solutions of Maxwell equations based on hybrid method combining generalized T-matrix and Foldy-Lax multiple scattering theory for vegetation/trees scattering," *2018 IEEE International Conference on Computational Electromagnetics (ICCEM)*, 2018.
38. Visser, T. D., D. G. Fischer, and E. Wolf, "Scattering of light from quasi-homogeneous sources by quasi-homogeneous media," *JOSA A*, Vol. 23, No. 7, 1631–1638, 2006.
39. Valagiannopoulos, C. A., "Closed-form solution to the scattering of a skew strip field by metallic PIN in a slab," *Progress In Electromagnetics Research*, Vol. 79, 1–21, 2008.
40. Asano, S. and G. Yamamoto, "Light scattering by a spheroidal particle," *Applied Optics*, Vol. 14, No. 1, 29–49, 1976.
41. Zhang, S. and J. M. Jin, *Computation of Special Functions*, Wiley, New York, 1996.
42. Li, L. W., X. K. Kang, and M. S. Leong, *Spheroidal Wave Functions in Electromagnetic Theory*, Wiley, New York, 2002.